



HAL
open science

Thermal effects on the mechanical behaviour of the soil-structure interface

Soheib Maghsoodi, O. Cuisinier, F. Masrouri

► **To cite this version:**

Soheib Maghsoodi, O. Cuisinier, F. Masrouri. Thermal effects on the mechanical behaviour of the soil-structure interface. Canadian Geotechnical Journal, 2019, 10.1139/cgj-2018-0583 . hal-02057063

HAL Id: hal-02057063

<https://hal.science/hal-02057063v1>

Submitted on 5 Mar 2019

HAL is a multi-disciplinary open access archive for the deposit and dissemination of scientific research documents, whether they are published or not. The documents may come from teaching and research institutions in France or abroad, or from public or private research centers.

L'archive ouverte pluridisciplinaire **HAL**, est destinée au dépôt et à la diffusion de documents scientifiques de niveau recherche, publiés ou non, émanant des établissements d'enseignement et de recherche français ou étrangers, des laboratoires publics ou privés.

1 Thermal effects on the mechanical behaviour of the 2 soil-structure interface

3 S.Maghsoodi^{1,2}, O.Cuisinier¹, F.Masrouri¹

4 ¹ *Université de Lorraine, CNRS, LEMTA, Nancy, France*

5 ² *École supérieure d'ingénieurs des travaux de la construction de Metz, Metz, France*

6 *Corresponding author: Soheib Maghsoodi (email: soheib.maghsoodi@univ-lorraine.fr)*

8 **Abstract**

9 The mechanical behaviour of the soil-structure interface plays a major role in the shear
10 characteristics and bearing capacity of foundations. In thermo-active structures, due to
11 non-isothermal conditions, the interface behaviour becomes more complex. The objective
12 of this study is to investigate the effects of temperature variations on the mechanical
13 behaviour of soils and soil-structure interface. Constant normal load (CNL) and constant
14 normal stiffness (CNS) tests were performed on soil and soil-structure interface in a direct
15 shear device at temperatures of 5, 22 and 60 °C. Fontainebleau sand and kaolin clay were
16 used as proxies for sandy and clayey soils. The sandy soil was prepared in a dense state,
17 and the clayey soil was prepared in a normally consolidated state. The results showed
18 that the applied thermal variations have a negligible effect on the shear strength of the
19 sand and sand-structure interface under CNL and CNS conditions, and the soil and soil-
20 structure interface behaviour could be considered thermally independent. In clay samples
21 the temperature increase, increased the cohesion and consequently the shear strength,
22 due to thermal contraction during heating. The temperature rise had less impact on the
23 shear strength in the case of the clay-structure interface than in the clay samples. The
24 adhesion of the clay-structure interface, is less than the cohesion of the clay samples.

25 **Keywords:** Shear strength, Constant normal stiffness (CNS), Soil-structure interface,
26 Temperature, Thermo-active structures.

27 **Résumé**

28 Le comportement mécanique de l'interface sol-structure est d'une grande importance en

29 raison du rôle de l'interface dans la résistance due au frottement et la capacité por-
30 tante des structures. Dans les structures thermo-actives du fait de la variation de la
31 température, le comportement de l'interface devient plus complexe. L'objectif de ce tra-
32 vail est d'étudier l'effet des variations de température sur le comportement mécanique
33 de l'interface sol-structure. Des essais avec des conditions de charge normale constante
34 (CNL) et de rigidité normale constante (CNS) ont été réalisées dans une boîte de cisaille-
35 ment direct à différentes températures, 5 °, 22 ° et 60 ° C sur des éprouvettes sol-sol et
36 sol-structure. Le sable de Fontainebleau et le kaolin ont été utilisés comme matériaux de
37 référence pour les sols sableux et argileux. Les résultats ont montré que les variations ther-
38 miques appliquées ont un effet négligeable sur la résistance au cisaillement des interfaces
39 sable-sable et sable-structure dans les conditions CNL et CNS et que le comportement
40 du sable peut être considéré comme étant indépendant de la température. Dans l'argile
41 étudiée, l'augmentation de la température augmente la résistance au cisaillement en rai-
42 son de la contraction thermique pendant le chauffage, ce qui augmente la cohésion du
43 sol. L'augmentation de température a eu moins d'impact sur la résistance au cisaillement
44 dans le cas de l'interface argile-structure que dans les échantillons argile. L'adhésion de
45 l'interface argile-structure est inférieure la cohésion de les échantillons d'argile.

46 **Mots clés:** Résistance au cisaillement, rigidité normale constante, interface sol-structure,
47 température, geostructures thermo-actives.

48

49 Introduction

50 The bearing capacity of foundations is highly dependent on the mechanical behaviour of
51 the soil-structure interface. Therefore, the soil-structure interactions at the interface are
52 of primary importance in foundation designs. Due to the recent developments of clean
53 energy, traditional geostructures such as piles and diaphragm walls have been converted
54 to energy geostructures by installing heat exchanger tubes inside the concrete element
55 ([Brandl 2006](#)). In energy geostructures the mechanical loads applied to the structure

56 on one hand, and the effect of heat exchange between structure and surrounding soil
57 on the other hand, modify the behaviour of the soil-structure interface. These thermal
58 variations and mechanical loads affect the bearing capacity and frictional resistance of
59 these thermo-active structures. Therefore, the effects of temperature on the soil-structure
60 interface mechanical parameters should be investigated. In this section, a state of the art
61 about the behaviour of the soil-structure interface and its influencing parameters under
62 isothermal conditions are presented. Then, existing studies on the effects of temperature
63 on the mechanical behaviour of soils and soil-structure interfaces are discussed.

64 Grain size, grain crushability, grain roundness, soil density, initial stress state, structure
65 roughness and shearing rate based on interface tests were addressed as the parameters
66 influencing the soil-structure interface mechanical behaviour (Potyondy 1961; Desai et al.
67 1985; Boulon and Foray 1986; Uesugi and Kishida 1986; Poulos and Al-Douri 1992;
68 Jardine et al. 1993; Lehane et al. 1993; Fakharian and Evgin 1997; Mortara 2001; Pra-Ai
69 2013).

70 An important concept to aid in understanding the interface behaviour is the constant
71 normal stiffness (CNS) conditions, which explains the real shear behaviour of embedded
72 foundations; as discussed in the following. The physical concept of constant normal
73 stiffness (CNS) conditions at the soil-structure interface, was introduced by Wernick 1978
74 (Fig. 1). Depending on the volumetric response of the soil at the interface during shearing
75 (dilative or contractive), the surrounding soil stiffness constrains the volumetric response
76 of the interface and acts as a virtual spring with a given stiffness (Eq. 1).

$$\Delta\sigma = -K.\Delta U \quad (1)$$

77 Where $\Delta\sigma$ (kPa) is the normal stress difference, K (kPa/mm) is the stiffness of the adjacent
78 soil (stiffness of the spring) and ΔU (mm) is the normal displacement difference of the
79 interface.

80 The tendency of the interface to dilate is counteracted by the elastic reaction of the
81 adjacent soil (Hoteit 1990; Tabucanon et al. 1995; Fioravante et al. 1999). Porcino et al.
82 2003 performed constant normal load (CNL) and constant normal stiffness (CNS) tests

83 on sand-steel interface and showed that the effect of the normal stiffness (K) on the mo-
 84 bilized shear resistance of the interfaces in CNS tests depends on the volumetric response
 85 exhibited by the interfaces in the CNL tests. They showed that in dilative regimes, the in-
 86 crease in the current normal stress (σ_n) when sheared in the CNS tests causes an increase
 87 in the current shear stress (τ). On the other hand, in the contractive regimes (smooth
 88 interface or loose soil), a decrease in the normal and shear stresses is observed. They
 89 also concluded that the increase or decrease in the mobilized shear resistance during the
 90 CNS tests are a consequence of the current normal stress evolution, and these changes in
 91 mobilized shear resistance are not an effect of the mobilized sand-structure friction angle
 92 modification, which remains unchanged.

93 Another important factor that influences the soil-structure interactions is the structure
 94 surface roughness (Kishida and Uesugi 1987; Porcino et al. 2003; Hu and Pu 2003).
 95 Normalized roughness (R_n), as reported by Uesugi and Kishida 1986, was defined by
 96 measuring R_{max} (vertical distance between the highest peak and lowest valley) along a
 97 profile length L equal to the mean grain size D_{50} and then normalized by D_{50} :

$$R_n = \frac{R_{max}(L = D_{50})}{D_{50}} \quad (2)$$

98 Previous investigations (Uesugi and Kishida 1986; Uesugi et al. 1989; Hu and Pu
 99 2003) indicate a range for the smooth and rough surfaces. The critical roughness ($R_{crit} =$
 100 $0.1 - 0.13$) was chosen as a range that ($R_n > R_{crit}$) is a rough surface and ($R_n < R_{crit}$)
 101 is considered as a smooth one.

102 The interface behaviour under non-isothermal conditions is a coupling between the
 103 above-mentioned parameters and temperature variations. In the following section, the
 104 thermal effects on the mechanical parameters of soils and the soil-structure interface are
 105 discussed. Different studies have been performed on the effects of temperature on the
 106 mechanical parameters of soils (Campanella and Mitchell 1968, Hueckel and Baldi 1990;
 107 Kuntiwattanakul et al. 1995; Burghignoli et al. 2000; Cui et al. 2000; Delage et al. 2000;
 108 Cekerevac and Laloui 2004; Abuel-Naga et al. 2006; Boukelia et al. 2017; Eslami et al.
 109 2017; Jarad et al. 2017), and these studies indicated that the thermo-mechanical be-

110 haviour of soils is highly dependent on the stress and thermal history of the material.
111 However, only a few studies have been performed on the soil-structure interactions under
112 non-isothermal conditions (Di Donna et al. 2015; Yavari et al. 2016). Di Donna et al. 2015
113 performed interface direct shear tests on quartz sand and illite clay at different tempera-
114 tures (22, 50 and 60 °C). These tests showed that the sand-concrete interface behaviour
115 was not directly affected by temperature changes, but the clay-concrete interface showed
116 higher shear strength at higher temperatures. The residual interface friction angle of the
117 clay-concrete decreased slightly at high temperatures, but the adhesion (cohesion between
118 soil and structure) increased with increasing temperature. The authors suggested that
119 this result is related to the thermal consolidation of the clay, which results in an increase
120 of the contact surface between the clay and concrete. Yavari et al. 2016 conducted soil-
121 structure interface direct shear tests on Fontainebleau sand and kaolin clay samples at
122 5, 20 and 40 °C. The shear strength of the clay samples was higher than that of the
123 clay-concrete interface, and the effects of temperature (in the range of 5-40 °C) on the
124 shear strength and friction angle were negligible in the sand, clay and clay-concrete in-
125 terface. They pre-consolidated all the samples to 100 kPa of vertical stress and heated
126 to 40 °C prior to the application of the initial conditions. Therefore, they found that the
127 effect of temperature on the clayconcrete interface, which was mainly related to thermal
128 consolidation, was negligible.

129 According to the literature, the effects of temperature on the friction angle and ad-
130 hesion of the soil-structure interface, are poorly understood under both CNL and CNS
131 conditions. In this study, a temperature-controlled direct shear device was used to per-
132 form interface tests on Fontainebleau sand and kaolin clay on a rough surface under CNL
133 and CNS conditions, to better understand the following:

- 134 • The effects of temperature on the shear strength (friction angle, cohesion and adhesion)
135 of soil and soil-structure interface under CNL and CNS conditions.
- 136 • The effect of surrounding soil stiffness on the soil-structure interface mechanical be-
137 haviour at different temperatures.
- 138 • The soil and soil-structure interface volumetric changes during heating (from 22 to 60

139 °C) and cooling (from 22 to 5 °C) under constant isotropic stress.

140 **Material properties, device and experimental programme**

141 In this section first, the materials used in this study are presented. Then, the details of
142 the temperature-controlled direct shear device, CNL and CNS tests with the device, and
143 calibration are discussed. Finally, the experimental programme is presented.

144 **Material properties**

145 The grain size distributions and physical properties of Fontainebleau sand (siliceous) and
146 kaolin clay used, in this study are presented in Fig. 2, Table 1 and Table 2.

147 To perform soil-structure interface direct shear tests, a stainless steel plate (80 x 60 x
148 10 mm) with the desired roughness was designed and used as the structure. This steel
149 plate is used to, avoid abrasion of the surface due to test repetition. The roughness of the
150 steel plate was measured with a laser profilometer (Fig. 3a). Four profiles with lengths
151 of 32 mm (Fig. 3b) parallel to the shear direction were measured. The heights of these
152 four profiles were obtained with the laser are presented in Fig. 4a. To determine the
153 roughness of the interface, each profile was divided into the D_{50} of Fontainebleau sand
154 (0.23 mm) and at each D_{50} , the R_{max} was measured. The values of R_{max} were divided
155 by D_{50} to obtain the normalized roughness (R_n). For Fontainebleau sand, the normalized
156 roughness R_n is presented in Fig. 4b. Most of the normalized values are between 0.02
157 and 0.3. The largest value of normalized roughness R_n (0.32) was determined; therefore,
158 the stainless steel plate is considered as a rough and very rough surface for Fontainebleau
159 sand and kaolin clay.

160 **Temperature-controlled direct shear device**

161 Fig. 5 shows the temperature-controlled direct shear device. The shear box (60 x 60
162 x 35 mm) was placed inside a container filled with water to reach saturated conditions
163 (Fig. 5). The heating system consisted of a heater that controlled the fluid temperature

164 circulating in the lower part of the container. Therefore, the water temperature in the
165 container reached the same temperature as the circulating fluid. Three thermocouples,
166 one in the lower half of the shear box, another on the upper half of the shear box and
167 the last in the container, controlled the applied temperature. In this direct shear device,
168 normal stress σ_n (kPa), shear displacement W (mm), circulating fluid temperature T ($^{\circ}C$)
169 and stiffness value K (kPa/mm) were applied, and normal displacement U (mm), shear
170 stress τ (kPa), and sample temperature T ($^{\circ}C$) were measured (Fig. 5).

171 **Constant normal load application**

172 To perform CNL tests, the normal load was applied with a loading frame and kept constant
173 during the tests. To start the shear, a shear displacement rate (mm/min) was applied to
174 the lower half of the shear box and the shear stress was measured. The different parts
175 of the device were connected to a data logger and a commanding system, which enabled
176 the operator to apply different thermo-mechanical paths. Calibrations were performed to
177 account for any temperature effects on different parts of the device.

178 **Constant normal stiffness application**

179 Under CNS conditions, two general behaviours are observed in soils: dilative (dense or
180 overconsolidated soils) and contractive (loose or normally consolidated soils). In the first
181 case, with starting the shear the soil at the interface starts to contract slightly ($\Delta U > 0$)
182 at the beginning of the test, and the amount of normal stress decreases (due to the
183 stiffness of the surrounding soil (virtual springs)) (Eq. 1). After this slight compression,
184 the soil starts to dilate ($\Delta U < 0$), and this dilation acts on the surrounding soil. Due
185 to the compression of the surrounding soil, the amount of the normal stress increases
186 ($\Delta\sigma > 0$). This normal stress rise, consequently increases the shear strength of the soil
187 at the interface. Conversely, in the second case (loose or normally consolidated soils), the
188 soil at the interface contracts ($\Delta U > 0$), and the normal stress decreases ($\Delta\sigma < 0$) until
189 the shear ceases.

190 To apply CNS condition to the temperature-controlled direct shear device, the follow-

191 ing procedure was implemented in the command software:

- 192 1. The total desired shear displacement, $W(8 \text{ mm})$ was divided into 100 segments
193 ($W/100 = 0.08 \text{ mm}$).
- 194 2. In order to reach the desired $W(8 \text{ mm})$ value: $(W/100) \times i \quad i = [1, 2, 3, \dots, 100]$
195 where i is the number of segments.
- 196 3. At the end of each segment, the device measures the vertical displacement difference
197 between the beginning of the segment and the end of the segment ($\Delta U = \Delta U_{i_2} - \Delta U_{i_1}$).
- 198 4. Then, according to Eq. 1, this difference ($\Delta U(mm)$) is multiplied by the value of
199 stiffness ($K \text{ (kPa/mm)}$), and the consequent normal stress ($\Delta \sigma_n$) that should be applied
200 is calculated.
- 201 5. This process is repeated for all segments $i(100)$ until the total shear displacement is
202 reached.

203 **Normal stiffness verification**

204 To calibrate the device for the stiffness application, the variations of normal stress ($\Delta \sigma$)
205 with normal displacement (ΔU) are presented in Fig. 6. The slope of these curves
206 represents the stiffness value. For tested values of stiffness, a satisfactory correlation is
207 obtained (1-2% precision).

208 **Experimental programme**

209 The experimental programme consisted of soil and soil-structure direct shear tests at dif-
210 ferent temperatures (Table 3). Soil tests were performed as reference cases for comparison
211 with soil-structure tests to better clarify the role of interface.

212 The sand programme consisted of a series of constant normal load (CNL) tests at
213 different temperatures to investigate the effects of temperature on the mechanical char-
214 acteristics. In sand-structure tests, CNL and CNS tests were performed at 22 and 60 °C.
215 For CNS tests, different stiffness values ($K = 500, 1000, \text{ and } 5000 \text{ kPa/mm}$) were chosen,
216 that were used in previous studies ([Boulon and Foray 1986](#); [Mortara 2001](#); [Pra-Ai 2013](#)).
217 Increasing the stiffness value restrains the volumetric response of the interface until a

218 certain case of constant normal stiffness which is called the constant volume condition
219 (CV). These values were chosen to cover the entire range of constant normal stiffness
220 conditions, from very small ranges close to CNL and up to very high values close to CV.
221 To perform the CNS tests, two scenarios were considered. First, shear tests with different
222 stiffness values ($K = 500, 1000, \text{ and } 5000 \text{ kPa/mm}$) and constant effective normal stress
223 ($\sigma'_{n0} = 100 \text{ kPa}$) were performed at 22 and 60 °C. The aim of this part was to determine
224 the effect of different stiffness values at 22 and 60 °C on sand-structure interface. The sec-
225 ond scenario, included interface shear tests at three different effective normal stress values
226 ($\sigma'_{n0} = 100, 200 \text{ and } 300 \text{ kPa}$) with a constant stiffness value ($K = 1000 \text{ kPa/mm}$). This
227 scenario was performed to determine the friction angle of the interface and also compare
228 the CNS and CNL tests.

229 **Sand programme**

230 To prepare the sand samples for the shear tests, the Fontainebleau sand with a target dry
231 density of 1.67 Mg/m^3 was poured into the shear box and compacted using a tamper.
232 This dry density corresponded to 90% of the relative density (D_r), and the sample was
233 considered to be a dense sand (Table 1). Then, the normal stress was applied to the sand
234 sample (path 0-1 in Fig. 7). After applying the normal stress, to shear the samples in
235 CNL condition at 22 °C, a shear rate of 0.1 mm/min was applied (path 1-2). For the
236 CNL tests at 60 °C, the heating phase (path 1-5, Fig. 7) was applied with a rate of 10
237 °C/hr, and the shearing phase (path 5-2') started.

238 For the sand-structure tests, the same procedure was performed, except the interface
239 was placed at the lower half of the shear box. For the sand-structure CNS tests, due to
240 the dense state of the soil, path 1-3 at 22 °C and path 5-3' at 60 °C were observed (Fig.
241 7).

242 **Clay programme**

243 To perform the clay and clay-structure shear tests, kaolin clay was prepared with a water
244 content of 63%, which was slightly higher than its liquid limit ($LL = 57\%$) and the

245 sample was left for 24 hours for homogenization. Subsequently, the clay was poured into
246 the shear box and special attention was paid to avoid any air trap. To perform the
247 CNL tests at 22 °C,, the normal stress was applied slowly and incrementally during the
248 consolidation phase, and each load increment lasted 2 hours, to ensure full consolidation
249 at each step (Mortezaie and Vucetic 2013). Two values of initial effective normal stresses
250 ($\sigma'_{n0} = 100, 300$ kPa) were chosen for the clay programme. Based on the consolidation tests
251 performed on this kaolin clay, the target void ratios after consolidation for $\sigma'_n = 100$ and
252 300 kPa were $e = 1$ and 0.85, respectively. After the consolidation phase for the CNL tests
253 at 22 °C, a displacement rate of 0.006 mm/min that was calculated from the settlement
254 curve and t_{50} (time required for the specimen to achieve 50 percent consolidation under the
255 maximum normal stress) of the kaolin, was applied (ASTM 1998). This slow rate ensured
256 drained conditions inside the shear box during shearing. The initial heating or cooling
257 phase started at ambient temperature (22 °C). After the consolidation phase, heating or
258 cooling was applied to the samples at a rate of 5 °C/hr. This slow rate avoids a pore
259 pressure increase during the heating phase and was verified by Cekerevac and Laloui 2004
260 and Di Donna et al. 2015. During the heating or cooling phase in the shear box, thermal
261 vertical deformation of the soil and the soil-structure interface was measured. After these
262 heating or cooling phases, the samples were sheared. For the CNL tests of the clay and
263 clay-structure interface, paths 1-2 and 5-2' were applied, as seen in Fig. 7, but for the
264 CNS clay-structure interface tests, paths 1-4 and 5-4' were observed due to the normally
265 consolidated state of the kaolin samples.

266 **Experimental results for sand**

267 In the following sections, first the CNL sand shear test results, and then, the CNL and
268 CNS sand-structure interface tests are discussed.

269 Sand

270 Fig. 8a presents the results of the sand CNL tests at 22 and 60 °C, which will be used as
271 a reference for the sand-structure tests. The dense sand samples show a peak shear stress
272 at a small shear displacement, and then, with a decrease, reach a critical state at both 22
273 and 60 °C. In Fig. 8b, the volumetric behaviour of the sand is presented. The amount
274 of contraction ($\Delta U > 0$) is around 0.06 mm; then, at 1.2 mm of shear displacement, the
275 dilation ($\Delta U < 0$) phase starts and continues until $U = -0.4$ mm, and finally, a constant
276 value corresponding to the critical state of the soil is reached. Fig. 8c shows the stress
277 ratio ($\eta = \tau/\sigma'_n$) variations with shear displacement, and the peak shear strengths are
278 reached at similar shear displacements ($W = 1.5 - 1.6$ mm) for different normal stresses.
279 Fig. 8d shows the Mohr-Coulomb plane for the sand samples. The peak friction angle for
280 the tests is 41.6° at 22 and 60 °C, while the residual friction angle is 34°. The same peak
281 and residual friction angles at both temperatures show the negligible effect of thermal
282 variations on the shearing behaviour of the studied sand.

283 Sand-structure

284 Constant normal load (CNL)

285 Fig. 9a shows the CNL results of the sand-structure tests with different initial effective
286 normal stresses ($\sigma'_{n0} = 100, 200, 300$ kPa) at 22 and 60 °C. The shear stress-shear dis-
287 placement curves reach peaks at approximately 1 mm of shear displacement, and then,
288 a sharp decrease of τ is observed. The peak and residual values of the shear stress at
289 different temperatures are almost the same. The contraction (0.01 mm) and dilation (-0.2
290 mm) amounts in the volumetric response are approximately half that of the sand case
291 due to the thickness of the soil sample in the sand-structure tests (Fig. 9b). In terms of
292 the temperature effects on the volumetric response, at both 22 and 60 °C, the volumetric
293 responses follow the same trend. The stress ratio curves for different temperatures vary
294 between 0.8-1 (Fig. 9c). The Mohr-Coulomb plane of the sand-structure tests under the
295 CNL condition is presented in Fig. 9d. The peak friction angle of the sand-structure

296 interface is 40.4° and the residual friction angle is 32.7° .

297 **Constant normal stiffness**

298 Fig. 10 shows the sand-structure interface CNS results for the first case ($\sigma'_{n0} = cte$ and
299 $K = 500, 1000, 5000$ kPa/mm). With increasing stiffness, the maximum shear strength for
300 CNS tests was increased due to the increase in normal stress (Fig. 10a). The CNS peak
301 shear stress obtained for larger shear displacements and the post-peak softening behaviour
302 was less evident than in the CNL sand-structure tests. In Fig. 10b, at the beginning
303 of shearing, the interface contracted slightly and then started to dilate. For $K = 500$
304 kPa/mm, the soil in the interface dilated approximately -0.2 mm, and by increasing the
305 stiffness to 5000 kPa/mm, the dilation was reduced to -0.08 mm (Fig. 10b). Increasing the
306 stiffness restrained the volumetric response of the soil at the interface. These restrained
307 dilations, increased the normal stress (Fig. 10c). The normal stress increased from the
308 initial value (100 kPa) to 180 kPa for $K = 500$ and 1000 kPa/mm. For $K = 5000$ kPa/mm
309 the normal stress increased to 510 kPa. Therefore, the normal stress variation during shear
310 depended on the volumetric response, and these normal stress increases, consequently
311 increase the shear stress acting on the interface. Fig. 10d shows the Mohr-Coulomb
312 plane of the sand-structure interface. All tests showed, with shear increase, the effective
313 normal stress decreased slightly at the beginning, then followed by an increase until the
314 end of shear. The comparison of curves at 22 and 60 °C shows that the temperature
315 has a negligible effect on the shearing behaviour of Fontainebleau sand-structure interface
316 under CNS conditions.

317 The second scenario ($\sigma'_{n0} = 100, 200, 300$ kPa and $K = cte$) results are reported in Fig.
318 11 and are compared with the results of the CNL case ($K = 0$ kPa/mm). The peak shear
319 stress for CNS tests were obtained for larger shear displacements (1.3 mm), compare to
320 CNL tests (0.8 mm). The increase in peak shear stress for $\sigma'_{n0} = 100, 200,$ and 300 kPa
321 in the CNS tests were $20, 60$ and 80 kPa respectively (Fig. 11a), compared to the values
322 on the CNL tests. The volumetric responses in the CNS tests are more restrained than
323 in CNL tests (Fig. 11b). In Fig. 11c, the normal stress variation during the CNS tests is

324 presented. The normal stress showed a slight decrease until 0.5 mm of $W(mm)$ and then
325 increased. This increase continued until 1.4 mm of $W(mm)$, which corresponds to the
326 peak shear stress; after this peak was reached, the normal stress remained unchanged. The
327 peak and residual friction angles of the interface in Fig. 11d are $\delta'_p = 37^\circ$ and $\delta'_{res} = 28^\circ$
328 which are smaller than the friction angles obtained in the sand tests (Fig. 8d). This point
329 confirms that the shear occurred exactly in the interface zone, and not in the soil mass.
330 [Pra-Ai 2013](#) conducted interface direct shear tests on dense Fontainebleau sand samples
331 on a rough steel plate under isothermal conditions, and they found 38° and 29° for the
332 peak and residual friction angles of the interface respectively. In the CNS sand-structure
333 interface tests, the peak and residual friction angle of the interface (40.7° and 32.4°) are
334 so close to those in the CNL sand-structure tests (40.4° and 32.7°). The friction angle of
335 the sand-structure interface is not affected by the CNS condition, which was also observed
336 by [Porcino et al. 2003](#).

337 **Sand vs. sand-structure interface**

338 In this section, the CNL test results for the sand and sand-structure interface are compared
339 to better understand the interface behaviour. The shear stress and volumetric response
340 in the CNL sand and sand-structure tests for $\sigma'_{n0}=100$ and 300 kPa at $T=22^\circ C$ are
341 compared in Fig. 12. In the sand-structure tests, the post-peak softening behaviour
342 is more pronounced than in the sand tests (Fig. 8). The peak shear stress is higher
343 (7-15%) in the sand samples than in the sand-structure tests, which confirms the shear
344 failure occurs in the interface zone. The peak shear stresses of the sand-structure tests are
345 obtained at smaller shear displacements (0.7-1 mm) than in the sand (1.6-1.8 mm) case,
346 which could be due to the rearrangement of grains in the interface zone ([Hoteit 1990](#),
347 [Tabucanon et al. 1995](#); [Porcino et al. 2003](#)).). The dilation phase began at smaller shear
348 displacements in the sand-structure interface tests (0.7 mm) than in the sand samples
349 (1.2 mm), and the amount of dilation (0.2 mm) was almost half that of the sand samples
350 (0.4 mm).

Experimental results for clay

This experimental section is divided into the clay and clay-structure results. For the clay tests, the CNL test results and for clay-structure interface tests, the CNL and CNS test results are discussed.

Clay

In this part first, thermal vertical strain of clay samples is presented. Second, the shear curves and volumetric responses for $\sigma'_{n0}=100$ and 300 kPa at 5, 22 and 60 °C are presented. To verify the repeatability of the results, the test with $\sigma'_{n0}=300$ kPa at 60 °C was repeated. After consolidation and reaching the desired void ratio, a heating or cooling phase at a rate of 5 °C/hr, was applied to the clay samples. This heating and cooling caused a thermal vertical deformation under constant effective normal stresses of 100 and 300 kPa (Fig. 13). The heating phase started from 22 to 60 °C and cooling phase was from 22 to 5 °C. The thermal vertical strain was higher for heating cases (0.6 – 0.64%) than cooling cases (0.18 – 0.2%). Therefore, the slope of heating curves was less than the cooling curves, and heating caused more contraction than cooling.

After heating or cooling, normally consolidated kaolin clay samples were sheared at two different effective normal stresses ($\sigma'_{n0}=100, 300$ kPa) at 5, 22 and 60 °C (Fig. 14). In Fig. 14a and c, the shear stress-shear displacement curves for 100 kPa and 300 kPa at 5, 22 and 60 °C are presented. As observed for both effective normal stresses, the shear stress increased with increasing temperature, until the peak values, then it decreased towards the critical state. The residual shear stresses at 5, 22 and 60 °C for $\sigma'_{n0}=100$ kPa became convergent after a shear displacement of 5 mm. For $\sigma'_{n0}=300$ kPa at 5 and 22 °C the shear stress increased in the same manner, but after a shear displacement of $W=3.5$ mm, the stress values diverged.

In the volumetric response, the samples that were exposed to higher temperatures showed less contraction during shear (Fig. 14b and Fig. 14d. For example in 100 kPa of effective normal stress, the test at 5 °C showed a contraction approximately 0.89 mm, but

378 for the tests at 22 and 60 °C, this amount decreased to approximately 0.68 mm and 0.38
379 mm respectively. For 300 kPa, the same trend was observed for the volumetric response
380 (Fig. 14d).

381 The Mohr-Coulomb plane for the clay tests at different temperatures is presented in
382 Fig. 15. The internal friction angle of the clay soil obtained at different temperatures,
383 shows a slight increase with temperature increase (14.4° to 15.3°) which can be considered
384 negligible, but the main difference was the cohesion increase from 11 to 17 kPa and then
385 to 23 kPa for tests at 5, 22 and 60 °C, which could be due to thermal hardening during
386 the heating phase.

387 Clay-structure

388 In the following sections, the CNL and CNS results for the clay-structure are presented.

389 Constant normal load (CNL)

390 Fig. 16 shows the thermal vertical strain for $\sigma'_{n0}=300$ kPa during the heating phase and
391 after consolidation. The thermal vertical strain caused by the temperature increase from
392 22 to 60 °C was approximately 0.85%, and for a temperature decrease from 22 to 5 °C in
393 the cooling case, the thermal vertical strain was approximately 0.2% for the clay-structure
394 interface tests.

395 The thermal volume deformation depends on the volume of the sample ([Campanella
396 and Mitchell 1968](#) and [Baldi et al. 1988](#)), and the thermal vertical strain is higher in the
397 clay-structure interface than in the clay samples due to the volume of the clay specimen
398 in the clay-structure tests.

399 In Fig. 17 the results of the clay-structure interface CNL tests are presented. Fig.
400 17a shows the shear stress versus shear displacement for $\sigma'_{n0}=100$ kPa. The peak shear
401 strength curve was slightly higher at 60 °C than at 5 and 22 °C ($\Delta\tau = 8$ kPa), but at the
402 critical state, all curves at different temperatures were superimposed. For $\sigma'_{n0}=300$ kPa
403 (Fig. 17c), the $\Delta\tau = 10$ kPa of difference at the peak was evident for 60 °C compared to
404 5 and 22 °C. In the critical state, the same behaviour as $\sigma'_{n0}=100$ kPa was observed.

405 In Fig. 17b and d the volumetric behaviours of the clay-structure interface are pre-
406 sented for $\sigma'_{n0}=100$ and 300 kPa. For $\sigma'_{n0}=100$ kPa (Fig. 17b), the amount of contraction
407 was 0.4 mm for the test at 5 °C, while it was 0.28 mm and 0.12 mm for the tests at 22
408 and 60 °C, respectively. For $\sigma'_{n0}=300$ kPa (Fig. 17d), the same behaviour was observed,
409 and the contraction at 5 °C was higher than those obtained at 22 and 60 °C.

410 Fig. 18 shows the Mohr-Coulomb plane for the clay-structure interface CNL tests at
411 different temperatures. The peak friction angle for all studied temperatures was 14°. The
412 main difference between the Mohr-Coulomb envelopes for different temperatures was the
413 adhesion. The increase in temperature, increased the peak adhesion (cohesion between
414 soil and structure) from 12.5 kPa to 18 kPa while the residual adhesion remained constant
415 (16.5 kPa).

416 **Constant normal stiffness (CNS)**

417 To investigate the shear characteristics of the clay-structure interface, constant normal
418 stiffness (CNS) conditions were applied. The results for $K = 1000$ kPa/mm that is
419 intermediate value between $K = 500$ (CNL) and 5000 kPa/mm (CV) are presented.

420 The shear stress versus shear displacement for two initial normal stresses ($\sigma'_{n0}=100$ and
421 300 kPa) at 22 and 60 °C are presented in Fig. 19a. At $\sigma'_{n0}=100$ kPa, the shear stress
422 increased with increasing shear displacement until reaching a value of 1 mm ($\tau = 33$ kPa)
423 then, with a slight decrease, the shear stress continued towards the critical state ($\tau = 28$
424 kPa). The curves for both 22 and 60 °C followed the same trend. Tests at $\sigma'_{n0}=300$ kPa
425 showed a very clear peak and then decreased towards a constant value. As mentioned for
426 100 kPa, under $\sigma'_{n0}=300$ kPa, the shear stresses at 22 and 60 °C are similar.

427 For both initial normal stresses, kaolin contracted until the end of the shear (Fig. 19b).
428 For $\sigma'_{n0}=100$ kPa at 22 °C, the amount of normal displacement in the critical state was
429 around 0.035 mm. This value was approximately 0.02 mm for tests at 60 °C, and the
430 heated samples showed less contraction. For $\sigma'_{n0}=300$ kPa at 22 and 60 °C, the amount
431 of normal displacement in the critical state was 0.9 and 0.6 mm, respectively.

432 In Fig. 19c the variation of normal stress during CNS tests of clay-structure interface is

433 presented. For both $\sigma'_{n0}=100$ and 300 kPa the normal stresses decreased during shearing
434 process. For samples exposed to higher temperatures the amount of reduction was less
435 than samples at 22 °C. For tests at $\sigma'_{n0}=100$ kPa at 22 and 60 °C the normal stress
436 decrease was about 42 and 30 kPa respectively.

437 In Fig. 19d, the normal stress vs. shear stress planes for the clay-structure interface
438 CNS and CNL tests are presented. For $\sigma'_{n0}=100$ and 300 kPa in the CNS tests, the
439 shear stress increased with decreasing normal stress, and the shear reached a peak value
440 and then decreased. The heated samples showed less decrease in the normal stress. For
441 example, for $\sigma'_{n0}=300$ kPa, the peak shear strength for heated samples was slightly higher
442 than 22 °C, and the normal stress decrease in the heated sample was also less than that
443 at 22 °C. The peak friction angle and adhesion of the CNS tests were 14° and 13 kPa
444 respectively.

445 **Clay vs. clay-structure interface**

446 In Fig. 20 the CNL tests of clay and clay-structure for $\sigma'_{n0}=100$ kPa are compared. The
447 peak shear stress in the clay-structure tests is obtained with smaller shear displacements
448 (1.2-1.6 mm), while for the clay, the peak shear stress is around (2.8-3.2 mm), and the
449 softening behaviour after the peak is more pronounced for the clay-structure interface.
450 The peak shear stress difference of 6 kPa for clay vs clay-structure at 22 °C and 7.5 kPa
451 at 60 °C for $\sigma'_{n0}=100$ kPa confirms that the shear occurs in the interface zone and not in
452 the soil mass.

453 In terms of volumetric behaviour, the clay tests are completely different with clay-
454 structure tests (Fig. 20b). In clay tests the contraction increases until the end of test but
455 in the clay-structure tests the contraction increases more rapidly compare to the clay tests,
456 and then remains constant. [Tsubakihara and Kishida 1993](#) have performed direct shear
457 tests on Kawasaki clay and mild steel. They found that, the reason for the volumetric
458 behaviour difference between clay and clay-structure tests, can be the sliding shear mode
459 that occurs in the interface.

460 Discussion

461 In the following section, the discussion about the effects of temperature on sand and clay
462 interface shear strength is presented.

463 Effect of temperature on sand

464 Fig. 21 shows the effect of temperature on cohesion, adhesion and friction angle of differ-
465 ent soils that have been studied for interface direct shear tests at different temperature
466 variations in the literature, which is compared to results obtained in this study. As can
467 be seen, the effect of temperature on the peak and residual friction angle of sand and
468 sand-structure interface are negligible (Fig. 21b). The similar shear curves, volumetric
469 behaviour and Mohr-Coulomb plane at different temperatures (Fig. 8) for sand samples
470 also confirm that, the effect of temperature on the shear strength of sand is negligible.
471 These observations are in line with existing studies ([Di Donna et al. 2015](#); [Yavari et al.](#)
472 [2016](#)). For sand-structure interface tests with different stiffness and temperatures, it was
473 observed that, the interface behaviour in CNS condition does not change at different tem-
474 peratures. For sandy soil used in this study, in the context of energy foundations, heating
475 a sand-structure interface in this range of temperatures does not change the mechanical
476 properties of the interface, and in the design calculations no further precautions should
477 be considered for thermal effects.

478 Effect of temperature on clay

479 In clay tests, heating under drained conditions led to a contraction of the samples, and
480 consequently the shear strength increased due to thermal hardening (Fig. 14). Several
481 authors observed this thermally induced contraction and shear strength increase during
482 drained heating of normally consolidated clays ([Campanella and Mitchell 1968](#); [Hueckel](#)
483 [and Baldi 1990](#); [Kuntiwattanakul et al. 1995](#); [Chiu 1996](#); [Cekerevac and Laloui 2004](#);
484 [Abuel-Naga et al. 2006](#)). [Baldi et al. 1988](#) have explained, the reason of this thermo-
485 plastic strain may be in the micro-structural changes as the tendency of clay flakes to

486 group together which increases the mineral-to-mineral contact and generates irreversible
487 strain.

488 Fig. 20 shows that the peak and residual shear strength in the clay-structure tests,
489 were always less than those obtained during clay tests. This showed that the shearing
490 occurred at the interface zone. Moreover, the peak shear stresses of the clay-structure
491 tests are close to the residual shear stress values of clay tests at all tested temperatures.
492 This may be due to the sliding, or partially sliding, shear mode along the interface.
493 Indeed, [Lemos and Vaughan 2000](#) showed that, in clays with high clay content in which
494 residual soil shear is in the sliding mode, peak interface shear strength normally is close
495 to the soil residual strength and is independent of roughness (Fig. 20). Therefore, in the
496 clay-structure interface tests performed in this study, the sliding or partially sliding shear
497 mode at interface occurred for all tested temperatures.

498 The peak cohesion of clay samples increases from 17 to 23 kPa while the peak adhesion
499 of clay-structure increases from 12 to 18 kPa with temperature increase from 22 to 60 °C
500 while the residual adhesion remained stable (Fig. 21a). Therefore, it can be concluded
501 that cohesion is more affected by temperature modification. This reflects the interaction
502 between the structure and the clay. For kaolin clay, heating the interface tend to slightly
503 increase the shear strength of the interface. Therefore, in terms of structural safety of
504 energy geostuctures, temperature increase in normally consolidated kaolin clay can be
505 considered as a positive aspect.

506 In isothermal conditions, [Potyondy 1961](#) have performed direct shear tests on different
507 soils and different structural materials like steel, concrete and wood. He found that
508 the friction angle and adhesion of a smooth steel interface is less than a smooth concrete
509 interface. Therefore, it can be concluded that the nature of the structural material plays a
510 major role in the interface behaviour and further works should be carried out to investigate
511 the nature the interface behaviour on different construction materials.

512 **Conclusions**

513 Constant normal load (CNL) and constant normal stiffness (CNS) interface tests were
514 conducted on soil and soil-structure samples at different temperatures (5,22 and 60 °C).
515 The results showed that the mechanical properties of sand are independent of temperature
516 (22 and 60 °C) for both sand and sand-structure tests. Different stiffness values were
517 applied under CNS conditions at different temperatures, and it was observed that such as
518 the CNL tests, the temperature does not change the interface behaviour under the CNS
519 condition. Additionally the same interface friction angle was obtained in both CNL and
520 CNS tests for sand-structure interface tests.

521 In kaolin clay, temperature does not affect the friction angle and the main effect is the
522 increase of the cohesion or adhesion. For clay tests, due to thermal contraction of kaolin
523 during heating, the soil becomes denser and shows a higher shear strength. It was found
524 that temperature increases the cohesion of clay samples. In clay-structure contact, due
525 to difference in the nature of materials (clay vs. metal) the adhesion is not as much
526 as clay case, therefore the shear strength increase with temperature increase, is not as
527 much as clay case. In CNS tests on clay-structure interface, the soil exposed to higher
528 temperatures, showed less contraction during shearing, and consequently less normal stress
529 decrease due to the denser state of the heated clay-structure samples prior to shearing.
530 Therefore, in the interface the soil becomes denser with heating and the shear strength
531 increases slightly.

532 Further work will be carried out to investigate the effects of thermo-mechanical cycling
533 on the mechanical behaviour of soil-structure interface.

References

- Abuel-Naga, H., Bergado, D., Ramana, G., Grino, L., Rujivipat, P. and Thet, Y., 2006. Experimental evaluation of engineering behavior of soft bangkok clay under elevated temperature, *Journal of geotechnical and geoenvironmental engineering*, **132**(7): 902–910.
- ASTM, 1998. Standard test method for direct shear test of soils under consolidated drained conditions, *ASTM standard D3080-98*, West Conshohocken, USA .
- Baldi, G., Hueckel, T. and Pellegrini, R., 1988. Thermal volume changes of the mineral–water system in low-porosity clay soils, *Canadian geotechnical journal* **25**(4): 807–825.
- Boukelia, A., Eslami, H., Rosin-Paumier, S. and Masrouri, F., 2017. Effect of temperature and initial state on variation of thermal parameters of fine compacted soils, *European Journal of Environmental and Civil Engineering* pp. 1–14.
- Boulon, M. and Foray, P., 1986. Physical and numerical simulation of lateral shaft friction along offshore piles in sand, *Proceedings of the 3rd International Conference on Numerical methods in Offshore piling, Nantes, France*, pp. 127–147.
- Brandl, H., 2006. Energy foundations and other thermo-active ground structures, *Géotechnique* **56**(2): 81–122.
- Burghignoli, A., Desideri, A. and Miliziano, S., 2000. A laboratory study on the thermomechanical behaviour of clayey soils, *Canadian Geotechnical Journal* **37**(4): 764–780.
- Campanella, R. G. and Mitchell, J. K., 1968. Influence of temperature variations on soil behavior, *Journal of Soil Mechanics and Foundations Division* **94**(SM3): 709–734.
- Cekerevac, C. and Laloui, L., 2004. Experimental study of thermal effects on the mechanical behaviour of a clay, *International journal for numerical and analytical methods in geomechanics* **28**(3): 209–228.
- Chiu, S.-L., 1996. Behaviour of normally consolidated clay at elevated temperature.
- Cui, Y. J., Sultan, N. and Delage, P., 2000. A thermomechanical model for saturated clays, *Canadian Geotechnical Journal* **37**(3): 607–620.
- Delage, P., Sultan, N. and Cui, Y. J., 2000. On the thermal consolidation of boom clay, *Canadian Geotechnical Journal* **37**(2): 343–354.
- Desai, C., Drumm, E. and Zaman, M., 1985. Cyclic testing and modeling of interfaces, *Journal of Geotechnical Engineering* **111**(6): 793–815.

- Di Donna, A., Ferrari, A. and Laloui, L., 2015. Experimental investigations of the soil–concrete interface: physical mechanisms, cyclic mobilization, and behaviour at different temperatures, *Canadian Geotechnical Journal* **53**(4): 659–672.
- Eslami, H., Rosin-Paumier, S., Abdallah, A. and Masrouri, F., 2017. Pressuremeter test parameters of a compacted illitic soil under thermal cycling, *Acta Geotechnica* **12**(5): 1105–1118.
- Fakharian, K. and Evgin, E., 1997. Cyclic simple-shear behavior of sand-steel interfaces under constant normal stiffness condition, *Journal of Geotechnical and Geoenvironmental Engineering* **123**(12): 1096–1105.
- Fioravante, V., Ghionna, V. N., Pedroni, S. and Porcino, D., 1999. A constant normal stiffness direct shear box for soil-solid interface tests, *Rivista Italiana di geotecnica* **33**(3): 7–22.
- Hoteit, 1990. *Etude expérimentale du comportement physique et mécanique des interfaces sols-structures*, PhD thesis, Institut National Polytechnique de Grenoble, Grenoble, France.
- Hu, L. and Pu, J. L., 2003. Application of damage model for soil–structure interface, *Computers and Geotechnics* **30**(2): 165–183.
- Hueckel, T. and Baldi, G., 1990. Thermoplasticity of saturated clays: experimental constitutive study, *Journal of geotechnical engineering* **116**(12): 1778–1796.
- Jarad, N., Cuisinier, O. and Masrouri, F., 2017. Effect of temperature and strain rate on the consolidation behaviour of compacted clayey soils, *European Journal of Environmental and Civil Engineering* pp. 1–18.
- Jardine, R., Lehane, B. and Everton, S., 1993. Friction coefficients for piles in sands and silts, *Offshore site investigation and foundation behaviour*, Springer, pp. 661–677.
- Kishida, H. and Uesugi, M., 1987. Tests of the interface between sand and steel in the simple shear apparatus, *Geotechnique* **37**(1): 45–52.
- Kuntiwattanakul, P., Towhata, I., Ohishi, K. and Seko, I., 1995. Temperature effects on undrained shear characteristics of clay, *Soils and Foundations* **35**(1): 147–162.
- Lehane, B., Jardine, R., Bond, A. J. and Frank, R., 1993. Mechanisms of shaft friction in sand from instrumented pile tests, *Journal of Geotechnical Engineering* **119**(1): 19–35.
- Lemos, L. and Vaughan, P., 2000. Clay–interface shear resistance, *Géotechnique* **50**(1): 55–64.

- Mortara, G., 2001. *An elastoplastic model for sand-structure interface behaviour under monotonic and cyclic loading*, PhD thesis, Technical University of Torino.
- Mortezaie, A. R. and Vucetic, M., 2013. Effect of frequency and vertical stress on cyclic degradation and pore water pressure in clay in the ngi simple shear device, *Journal of Geotechnical and Geoenvironmental Engineering* **139**(10): 1727–1737.
- Porcino, D., Fioravante, V., Ghionna, V. N. and Pedroni, S., 2003. Interface behavior of sands from constant normal stiffness direct shear tests, *Geotechnical Testing Journal* **26**(3): 289–301.
- Potyondy, J. G., 1961. Skin friction between various soils and construction materials, *Geotechnique* **11**(4): 339–353.
- Poulos, H. and Al-Douri, R., 1992. Influence of soil density on pile skin friction in calcareous sediments, *Proc., 6th ANZ Conf. on Geomech*, pp. 375–380.
- Pra-Ai, S., 2013. *Behaviour of soil-structure interfaces subjected to a large number of cycles. Application to piles*, PhD thesis, University of Grenoble Alpes, Grenoble, France.
- Tabucanon, J. T., Airey, D. W. and Poulos, H. G., 1995. Pile skin friction in sands from constant normal stiffness tests.
- Tsubakihara, Y. and Kishida, H., 1993. Frictional behaviour between normally consolidated clay and steel by two direct shear type apparatuses, *Soils and Foundations* **33**(2): 1–13.
- Uesugi, M. and Kishida, H., 1986. Frictional resistance at yield between dry sand and mild steel, *Soils and foundations* **26**(4): 139–149.
- Uesugi, M., Kishida, H. and Tsubakihara, Y., 1989. Friction between sand and steel under repeated loading, *Soils and foundations* **29**(3): 127–137.
- Wernick, E., 1978. Skin friction of cylindrical anchors in non-cohesive soils, *Symposium on Soil Reinforcing and Stabilising Techniques in Engineering Practice* **42**(42): 201219.
- Yavari, N., Tang, A. M., Pereira, J.-M. and Hassen, G., 2016. Effect of temperature on the shear strength of soils and the soil–structure interface, *Canadian Geotechnical Journal* **53**(7): 1186–1194.

List of symbols

- CNL Constant normal load
- CNS Constant normal stiffness
- $K(kPa/mm)$ Imposed normal stiffness
- $\tau(kPa)$ Shear stress
- $\sigma'_n(kPa)$ Effective normal stress
- $U(mm)$ Normal displacement
- $W(mm)$ Shear displacement
- $R_{max}(mm)$ Maximum surface roughness
- $R_n(-)$ Normalized surface roughness
- $\delta'_p(^{\circ})$ Peak friction angle of interface
- $\delta'_{res}(^{\circ})$ Residual friction angle of interface
- $\phi'_p(^{\circ})$ Peak friction angle of soil
- $\phi'_{res}(^{\circ})$ Residual friction angle of soil
- $C'_p(^{\circ})$ Peak cohesion of soil
- $C'_{i,p}(^{\circ})$ Peak adhesion of soil-structure
- $D_{50}(mm)$ mean diameter of soil particles
- $\rho_s(g/cm^3)$ grain density of soil particles
- $\gamma_{dmax}(kN/m^3)$ maximum dry density
- $\gamma_{dmin}(kN/m^3)$ minimum dry density
- e_{max} maximum void ratio
- e_{min} minimum void ratio
- $C_u = D_{60}/D_{10}$ coefficient of uniformity
- $k(m/s)$ hydraulic conductivity

List of Tables

1 Fontainebleau sand physical properties 26

2 Kaolin clay physical and thermal properties 27

3 Experimental programme of soil and soil-structure interface tests 28

Table 1: Fontainebleau sand physical properties (Pra-Ai 2013)

D_{50} (mm)	ρ_s (g/cm ³)	γ_{dmax} (kN/m ³)	γ_{dmin} (kN/m ³)	e_{max}	e_{min}	$C_u = \frac{D_{60}}{D_{10}}$
0.23	2.65	17.2	14.2	0.866	0.545	1.72

Table 2: Kaolin clay physical and thermal properties (Yavari et al. 2016)

LL (%)	PL (%)	I_p (%)	ρ_s (Mg/m^3)	λ (W/mK)	C (J/m^3K)	k (m/s)
57	33	24	2.60	1.5	3.3	10^{-8}

Table 3: Experimental programme of soil and soil-structure interface tests

	$\sigma_n(kPa)$	$K (kPa/mm)$	$T^\circ(C)$	Type of test
Sand	100, 200, 300	0	22°	CNL
Sand	100, 200, 300	0	60°	CNL
Sand-structure	100, 200, 300	0	22°	CNL
Sand-structure	100, 200, 300	0	60°	CNL
Sand-structure	100	500, 1000, 5000	22°	CNS
Sand-structure	100	500, 1000, 5000	60°	CNS
Sand-structure	100, 200, 300	1000	22°	CNS
Clay	100, 300	0	5°	CNL
Clay	100, 300	0	22°	CNL
Clay	100, 300	0	60°	CNL
Clay-structure	100, 300	0	5°	CNL
Clay-structure	100, 300	0	22°	CNL
Clay-structure	100, 300	0	60°	CNL
Clay-structure	100, 300	1000	22°	CNS
Clay-structure	100, 300	1000	60°	CNS

List of Figures

1	CNS concept of the soil-structure interface (after Wernick 1978).	31
2	Grain size distribution of Fontainebleau sand and kaolin clay.	32
3	(a) Steel mould dimensions and, laser setup (b) direction and dimensions of laser profiles.	33
4	(a) Measured profiles (b) normalized roughness measurements for each profile length ($L = D_{50}$).	34
5	Experimental setup of the direct shear temperature-controlled device.	35
6	Imposed stiffness verification. (a) $K = 500$ kPa/mm; (b) $K = 1000$ kPa/mm; (c) $K = 5000$ kPa/mm. $\sigma'_{n0} = 100$ kPa.	36
7	Thermo-mechanical path in this study.	37
8	CNL results for sand samples at $T = 22^{\circ}C$ and $T = 60^{\circ}C$. (a) Shear stress vs. shear displacement; (b) normal displacement vs. shear displacement; (c) stress ratio vs. shear displacement; (d) shear stress vs. effective normal stress	38
9	CNL results for sand-structure interface at $T = 22^{\circ}C$ and $T = 60^{\circ}C$. (a) Shear stress vs. shear displacement; (b) normal displacement vs. shear displacement; (c) stress ratio vs. shear displacement; (d) shear stress vs. effective normal stress	39
10	CNS results for sand-structure interface at $T = 22^{\circ}C$ and $T = 60^{\circ}C$ for same initial normal stress (100 kPa). (a) Shear stress vs. shear displacement; (b) normal displacement vs. shear displacement; (c) normal stress vs. shear displacement; (d) shear stress vs. effective normal stress	40
11	Comparison of CNS and CNL ($K = 0$ kPa/mm) results for sand-structure interface at $T = 22^{\circ}C$ for different initial normal stresses (100,200,300 kPa) and $K = 1000$ kPa/mm. (a) Shear stress vs. shear displacement; (b) normal displacement vs. shear displacement; (c) effective normal stress vs. shear displacement; (d) shear stress vs. effective normal stress	41
12	Comparison of CNL results for sand and sand-structure with $\sigma'_{n0} = 100$ and 300 kPa at $T = 22^{\circ}C$	42
13	Thermal vertical strain of clay samples during heating and cooling phase. Heating or cooling rate: $5^{\circ}C/hr$	43
14	CNL results for clay samples at $T = 22^{\circ}C$, $T = 60^{\circ}C$ and $T = 5^{\circ}C$. (a) Shear stress vs. shear displacement ($\sigma'_{n0} = 100$ kPa); (b) normal displacement vs. shear displacement ($\sigma'_{n0} = 100$ kPa); (c) shear stress vs. shear displacement ($\sigma'_{n0} = 300$ kPa); (d) normal displacement vs. shear displacement ($\sigma'_{n0} = 300$ kPa)	44

15	Shear stress vs. effective normal stress of CNL clay tests at $T = 5\text{ }^{\circ}\text{C}$, $T = 22\text{ }^{\circ}\text{C}$ and $T = 60\text{ }^{\circ}\text{C}$	45
16	Thermal vertical strain of clay-structure interface during heating and cooling phase. Heating or cooling rate: $5\text{ }^{\circ}\text{C}/\text{hr}$	46
17	CNL results for clay-structure interface at $T = 5\text{ }^{\circ}\text{C}$, $T = 22\text{ }^{\circ}\text{C}$ and $T = 60\text{ }^{\circ}\text{C}$. (a) Shear stress vs. shear displacement ($\sigma'_{n0} = 100\text{ kPa}$); (b) normal displacement vs. shear displacement ($\sigma'_{n0} = 100\text{ kPa}$); (c) shear stress vs. shear displacement ($\sigma'_{n0} = 300\text{ kPa}$); (d) normal displacement vs. shear displacement ($\sigma'_{n0} = 300\text{ kPa}$)	47
18	Shear stress vs. effective normal stress of CNL tests of clay-structure interface at $T = 5\text{ }^{\circ}\text{C}$, $T = 22\text{ }^{\circ}\text{C}$ and $T = 60\text{ }^{\circ}\text{C}$	48
19	CNS results for clay-structure interface at $T = 22\text{ }^{\circ}\text{C}$, $T = 60\text{ }^{\circ}\text{C}$. (a) shear stress vs. shear displacement; (b) Normal displacement vs. shear displacement; (c) Normal stress vs. shear displacement; (d) shear stress vs. effective normal stress	49
20	Comparison of CNL results for clay and clay-structure interface with $\sigma'_{n0} = 100\text{ kPa}$ at $T = 5\text{ }^{\circ}\text{C}$, $T = 22\text{ }^{\circ}\text{C}$ and $T = 60\text{ }^{\circ}\text{C}$	50
21	Effect of temperature on (a) cohesion and (b) friction angle.	51

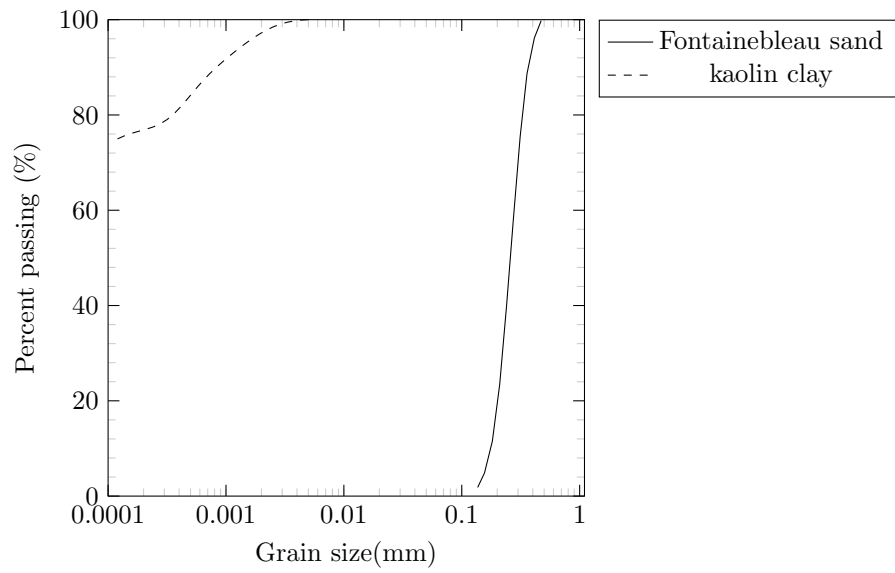


Figure 2: Grain size distribution of Fontainebleau sand and kaolin clay.

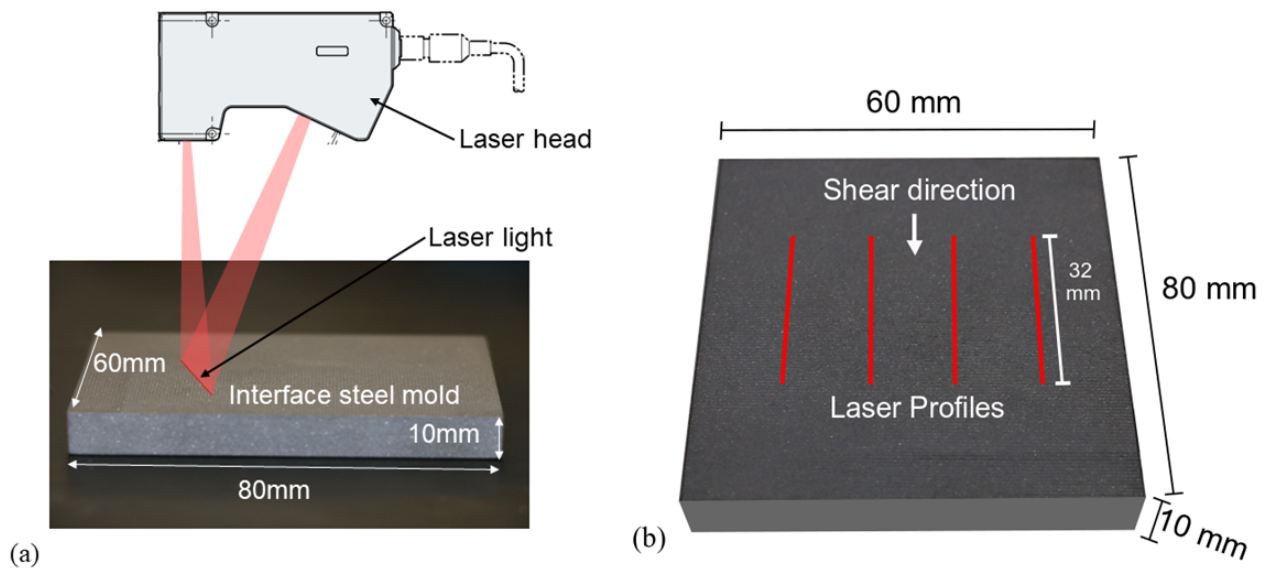


Figure 3: (a) Steel mould dimensions and, laser setup (b) direction and dimensions of laser profiles.

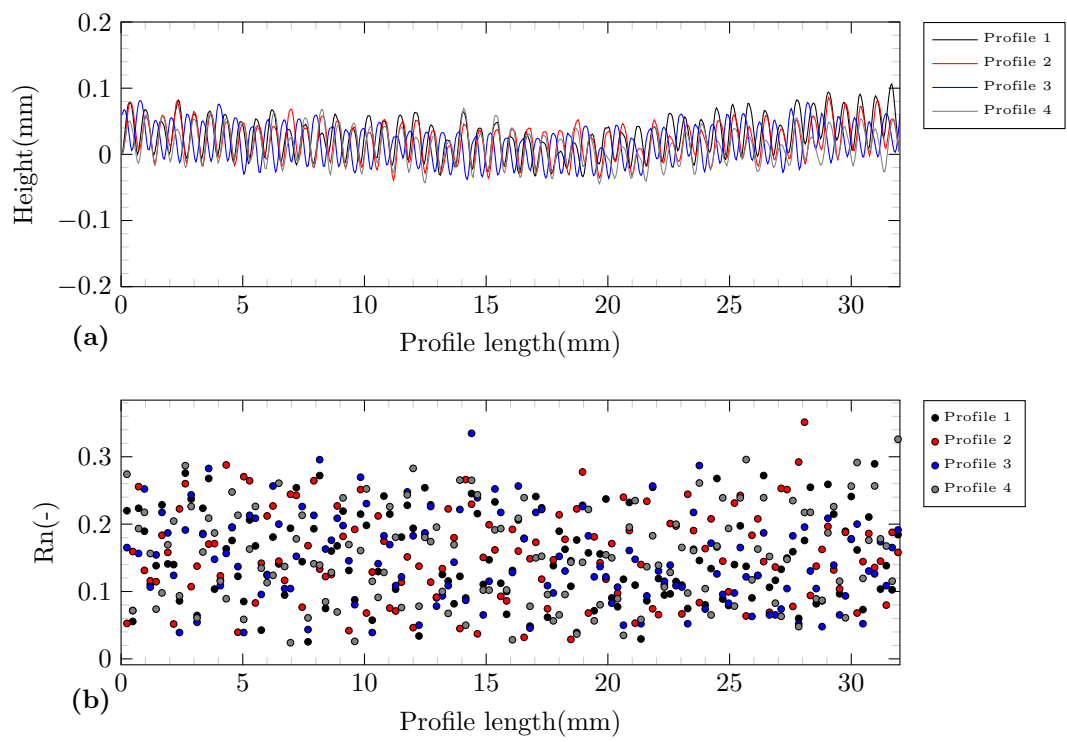


Figure 4: (a) Measured profiles (b) normalized roughness measurements for each profile length ($L = D_{50}$).

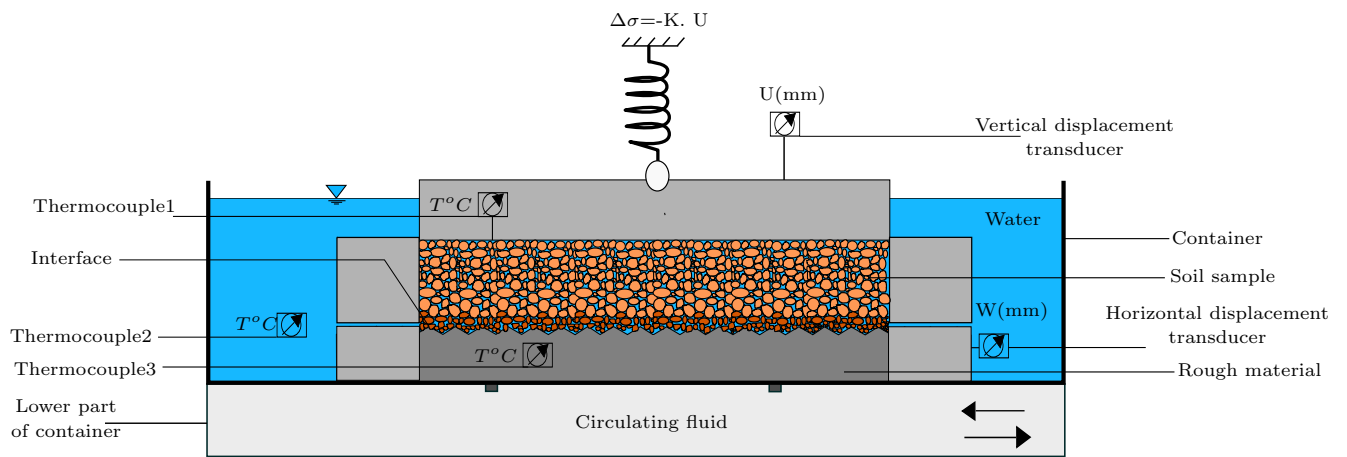


Figure 5: Experimental setup of the direct shear temperature-controlled device.

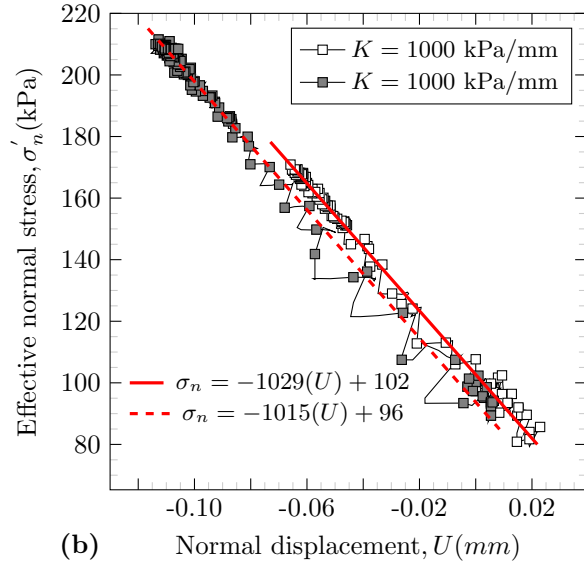
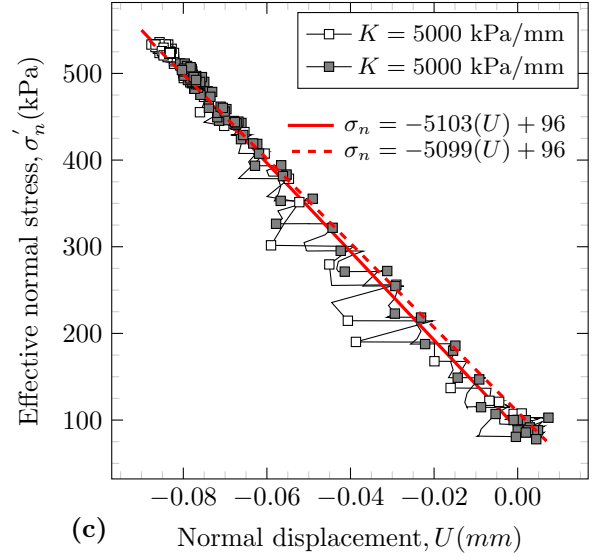
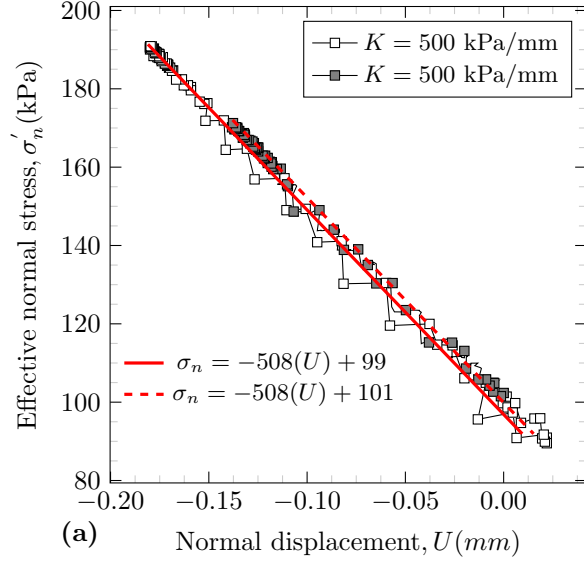


Figure 6: Imposed stiffness verification. (a) $K = 500$ kPa/mm; (b) $K = 1000$ kPa/mm; (c) $K = 5000$ kPa/mm. $\sigma'_{n0} = 100$ kPa.

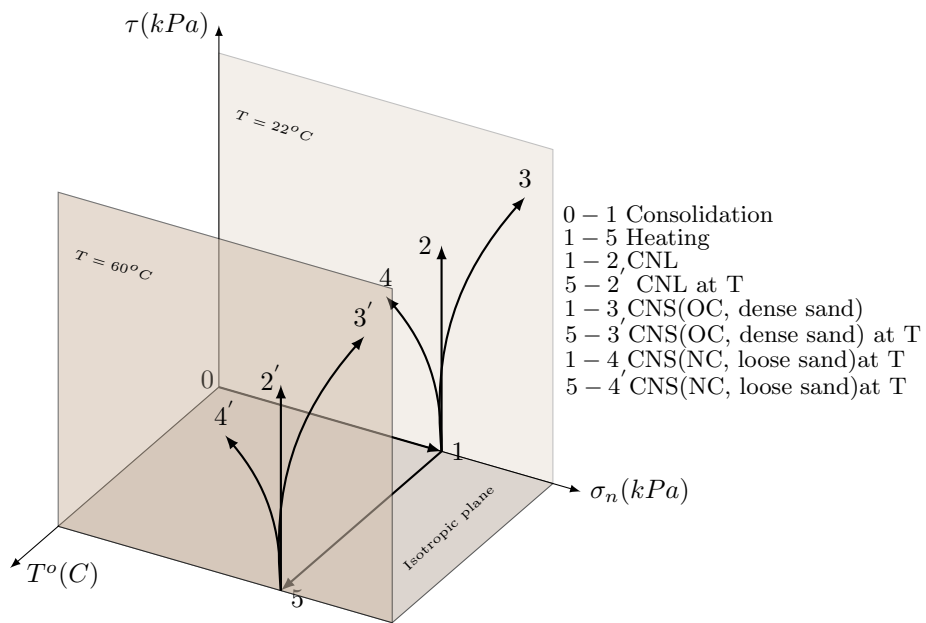


Figure 7: Thermo-mechanical path in this study.

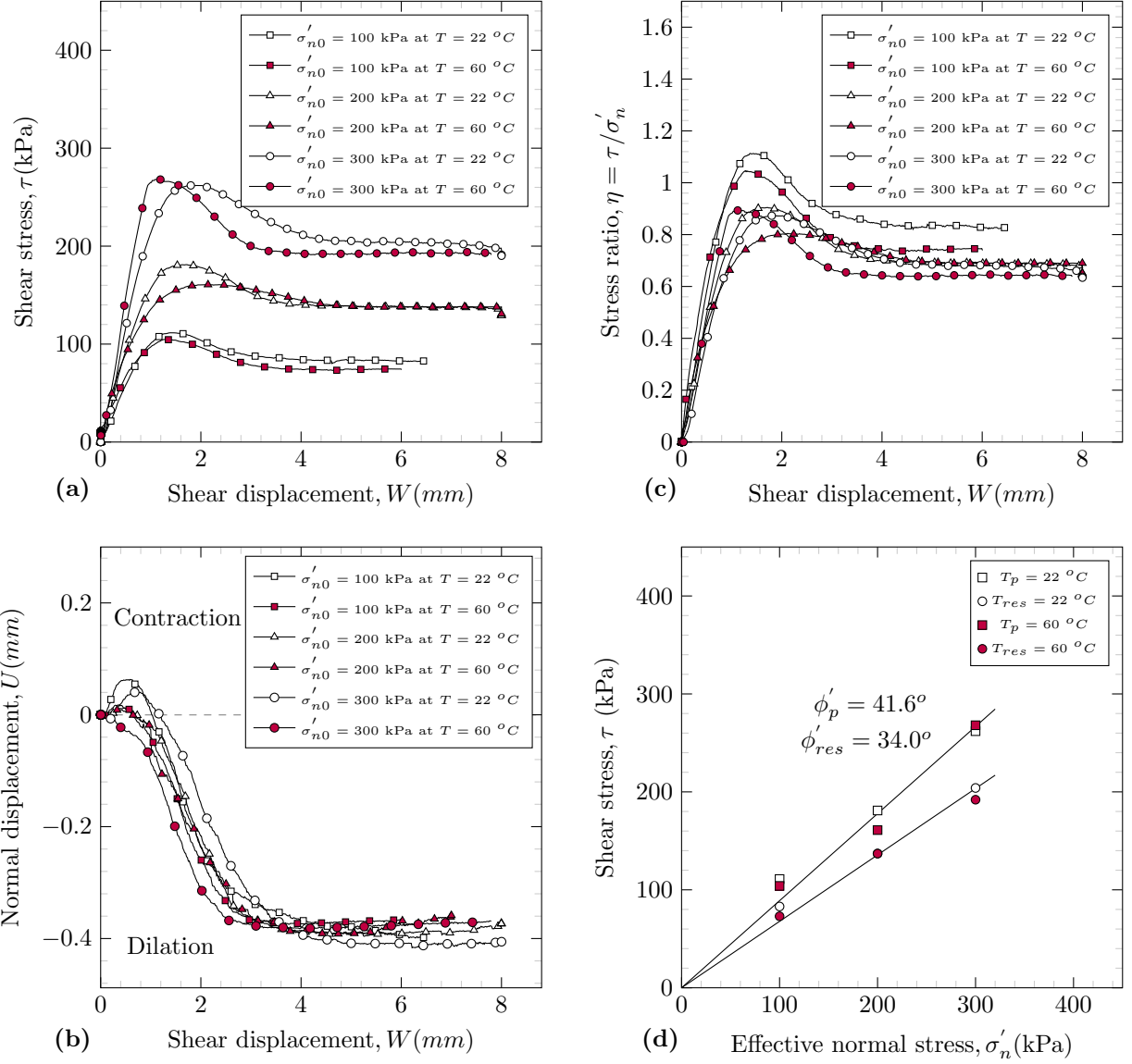


Figure 8: CNL results for sand samples at $T = 22^\circ\text{C}$ and $T = 60^\circ\text{C}$. (a) Shear stress vs. shear displacement; (b) normal displacement vs. shear displacement; (c) stress ratio vs. shear displacement; (d) shear stress vs. effective normal stress

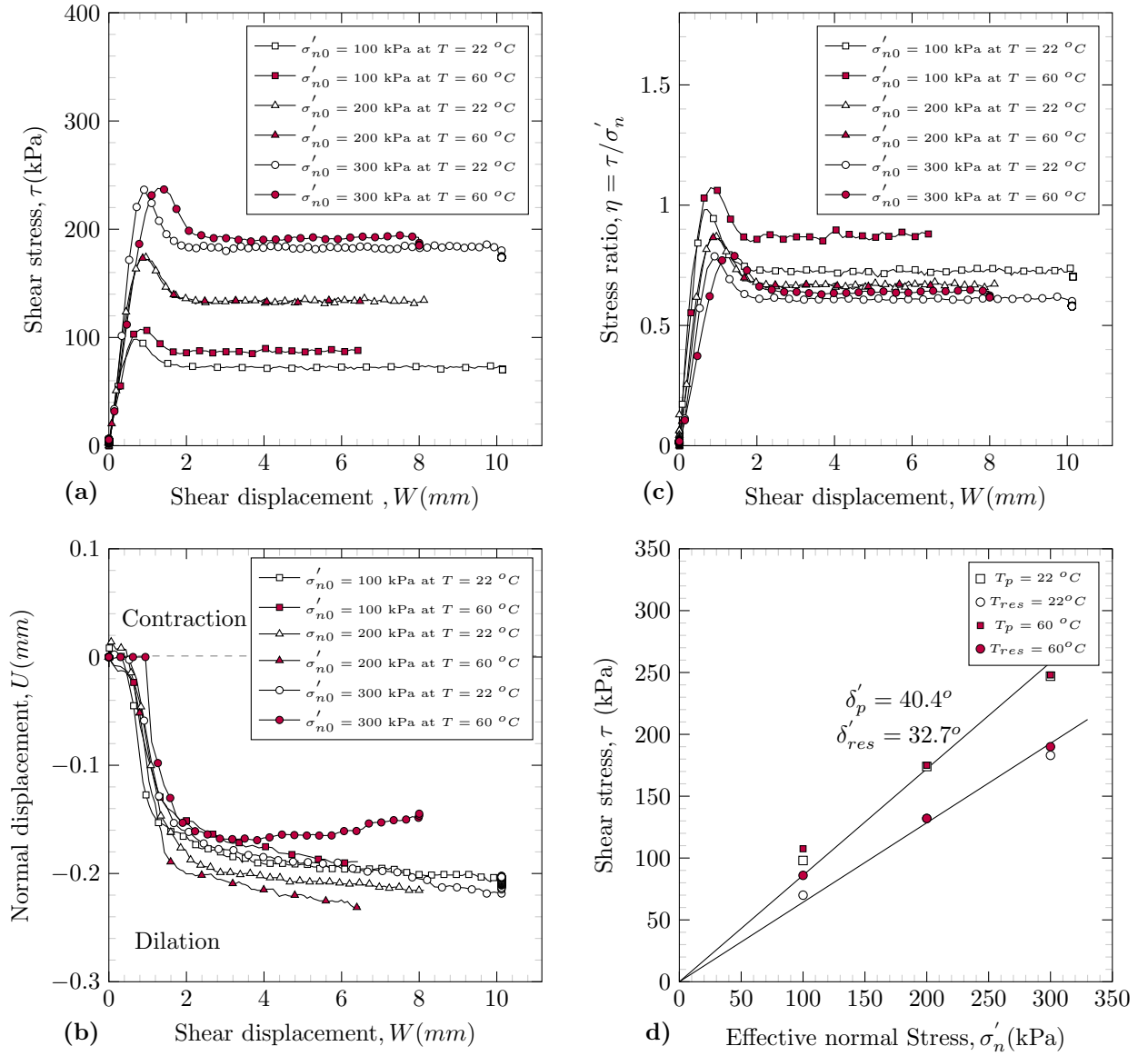


Figure 9: CNL results for sand-structure interface at $T = 22^\circ\text{C}$ and $T = 60^\circ\text{C}$. (a) Shear stress vs. shear displacement; (b) normal displacement vs. shear displacement; (c) stress ratio vs. shear displacement; (d) shear stress vs. effective normal stress

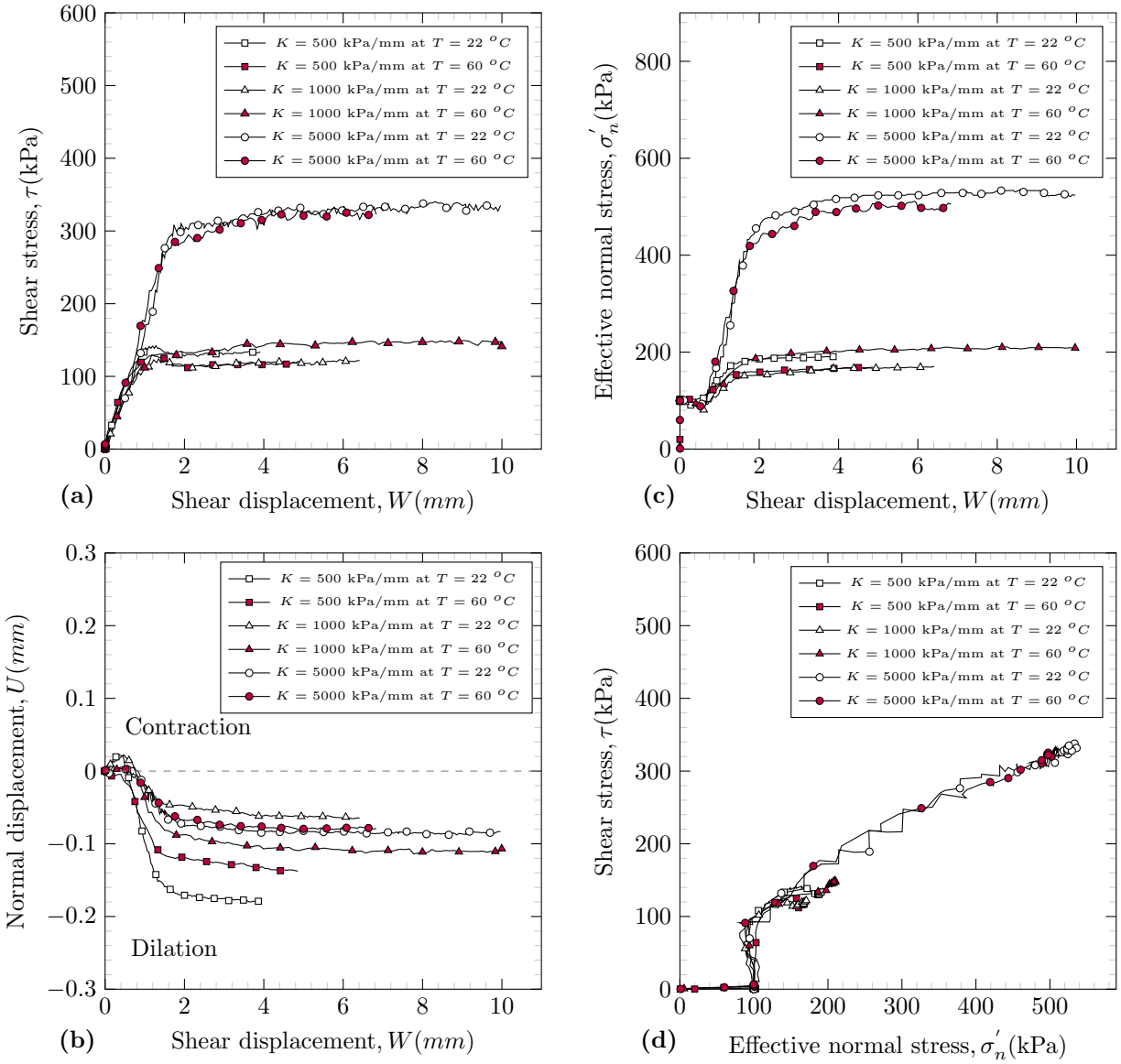


Figure 10: CNS results for sand-structure interface at $T = 22^\circ\text{C}$ and $T = 60^\circ\text{C}$ for same initial normal stress (100 kPa). (a) Shear stress vs. shear displacement; (b) normal displacement vs. shear displacement; (c) normal stress vs. shear displacement; (d) shear stress vs. effective normal stress

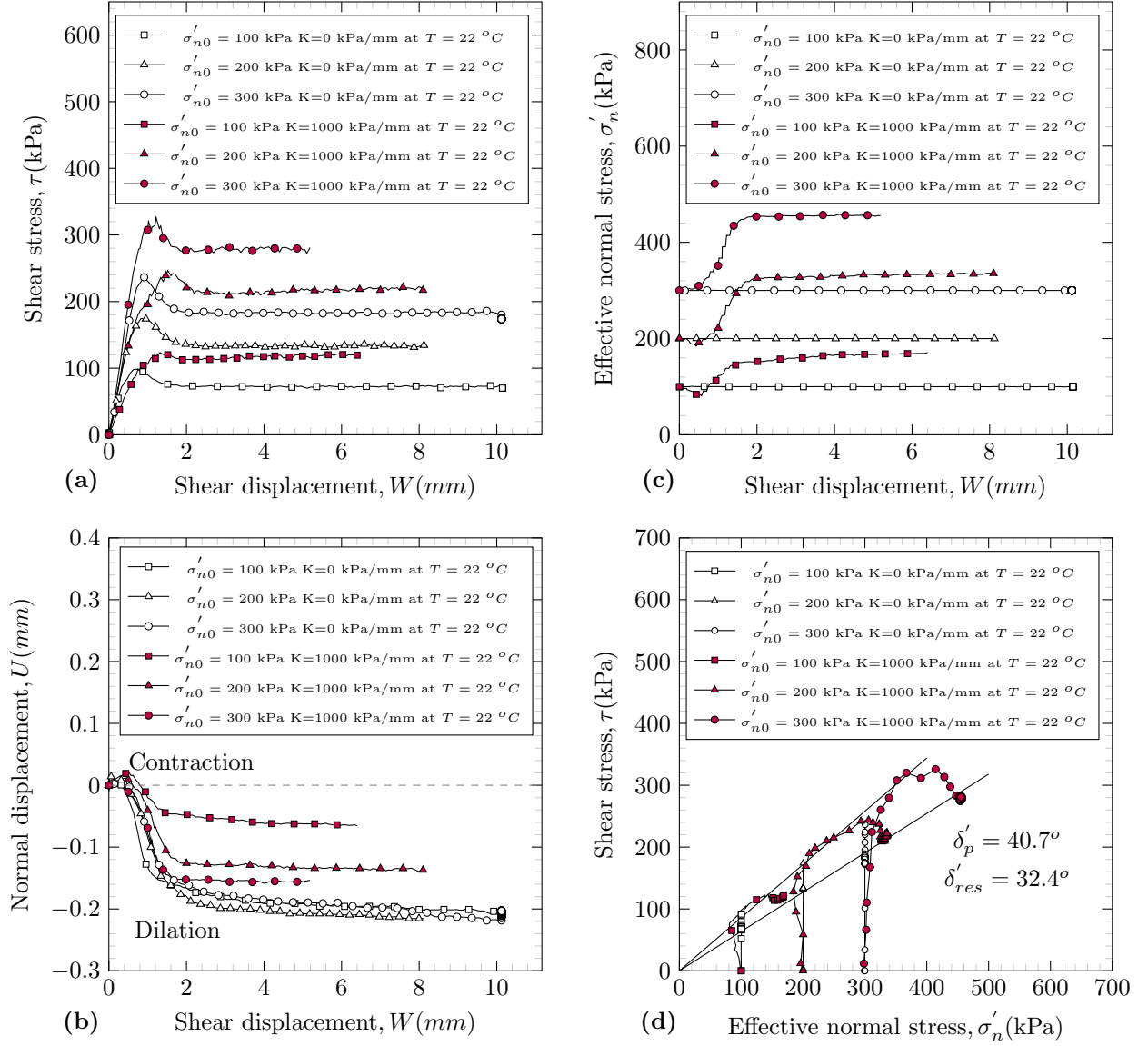


Figure 11: Comparison of CNS and CNL ($K = 0$ kPa/mm) results for sand-structure interface at $T = 22^\circ\text{C}$ for different initial normal stresses (100,200,300 kPa) and $K = 1000$ kPa/mm. (a) Shear stress vs. shear displacement; (b) normal displacement vs. shear displacement; (c) effective normal stress vs. shear displacement; (d) shear stress vs. effective normal stress

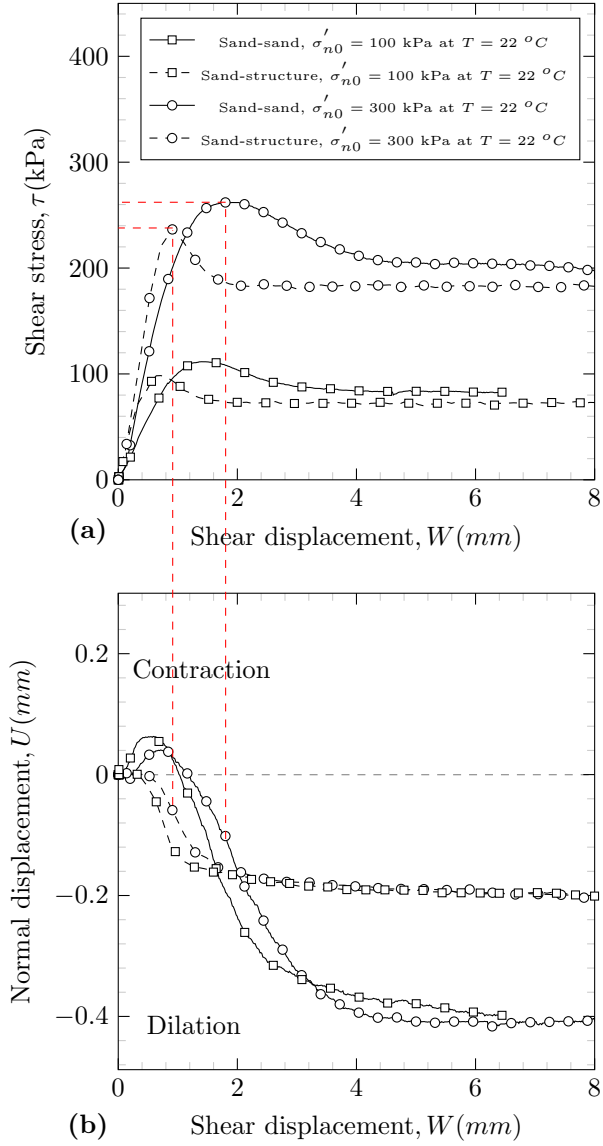


Figure 12: Comparison of CNL results for sand and sand-structure with $\sigma'_{n0} = 100$ and 300 kPa at $T = 22$ °C.

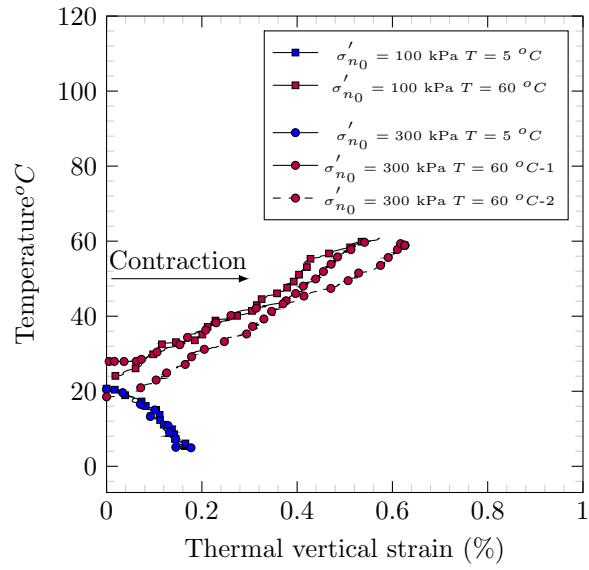


Figure 13: Thermal vertical strain of clay samples during heating and cooling phase. Heating or cooling rate: 5 °C/hr

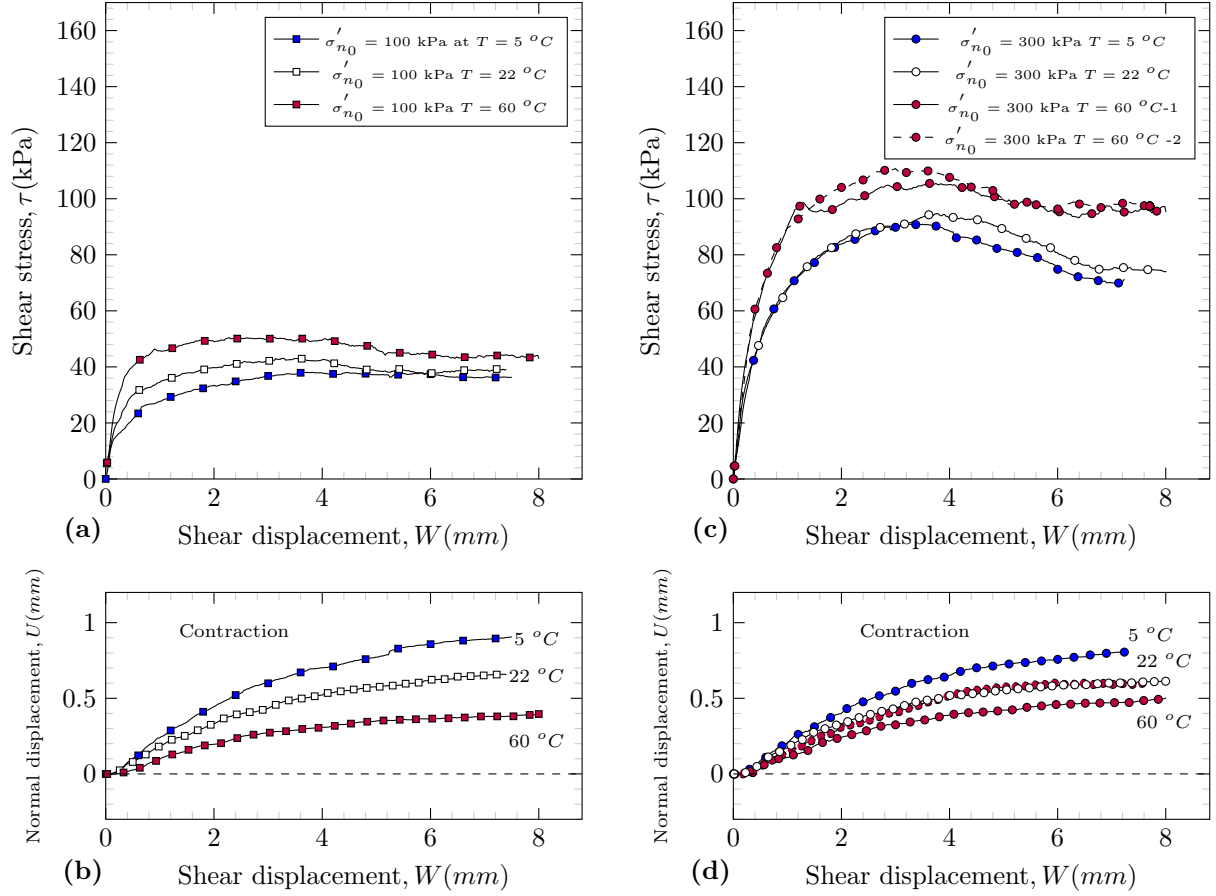


Figure 14: CNL results for clay samples at $T = 22$ °C, $T = 60$ °C and $T = 5$ °C. (a) Shear stress vs. shear displacement ($\sigma'_{n0} = 100$ kPa); (b) normal displacement vs. shear displacement ($\sigma'_{n0} = 100$ kPa); (c) shear stress vs. shear displacement ($\sigma'_{n0} = 300$ kPa); (d) normal displacement vs. shear displacement ($\sigma'_{n0} = 300$ kPa)

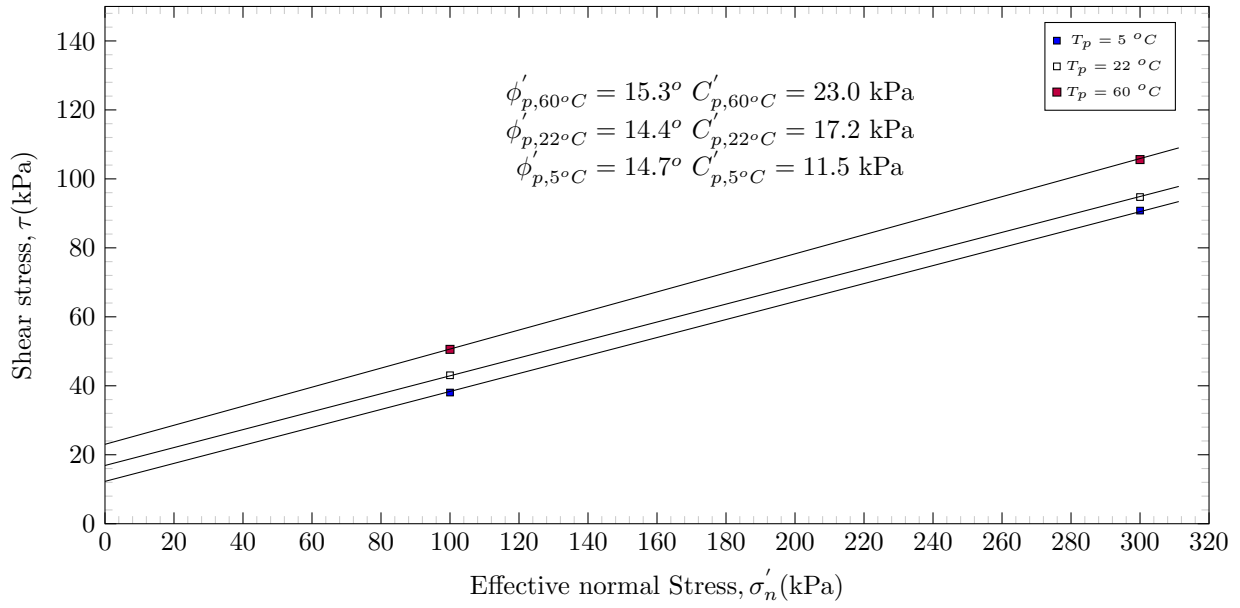


Figure 15: Shear stress vs. effective normal stress of CNL clay tests at $T = 5^{\circ}C$, $T = 22^{\circ}C$ and $T = 60^{\circ}C$

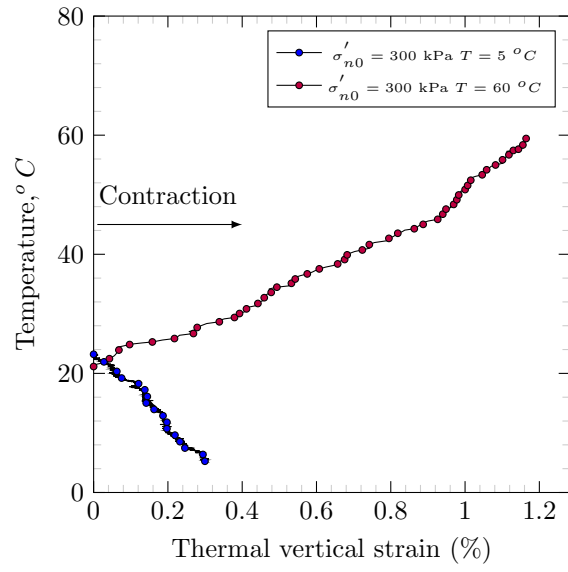


Figure 16: Thermal vertical strain of clay-structure interface during heating and cooling phase. Heating or cooling rate: 5 °C/hr

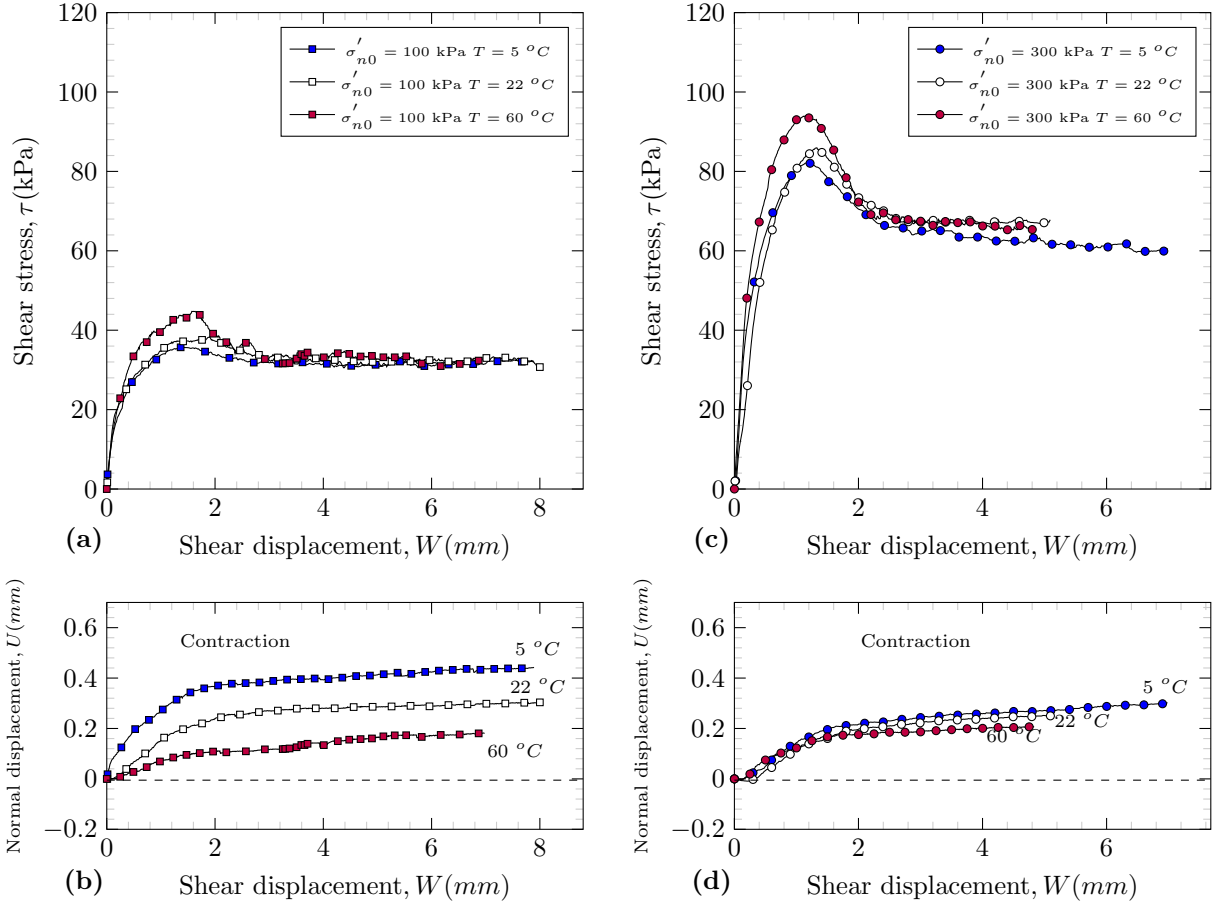


Figure 17: CNL results for clay-structure interface at $T = 5^\circ\text{C}$, $T = 22^\circ\text{C}$ and $T = 60^\circ\text{C}$. (a) Shear stress vs. shear displacement ($\sigma'_{n0} = 100$ kPa); (b) normal displacement vs. shear displacement ($\sigma'_{n0} = 100$ kPa); (c) shear stress vs. shear displacement ($\sigma'_{n0} = 300$ kPa); (d) normal displacement vs. shear displacement ($\sigma'_{n0} = 300$ kPa)

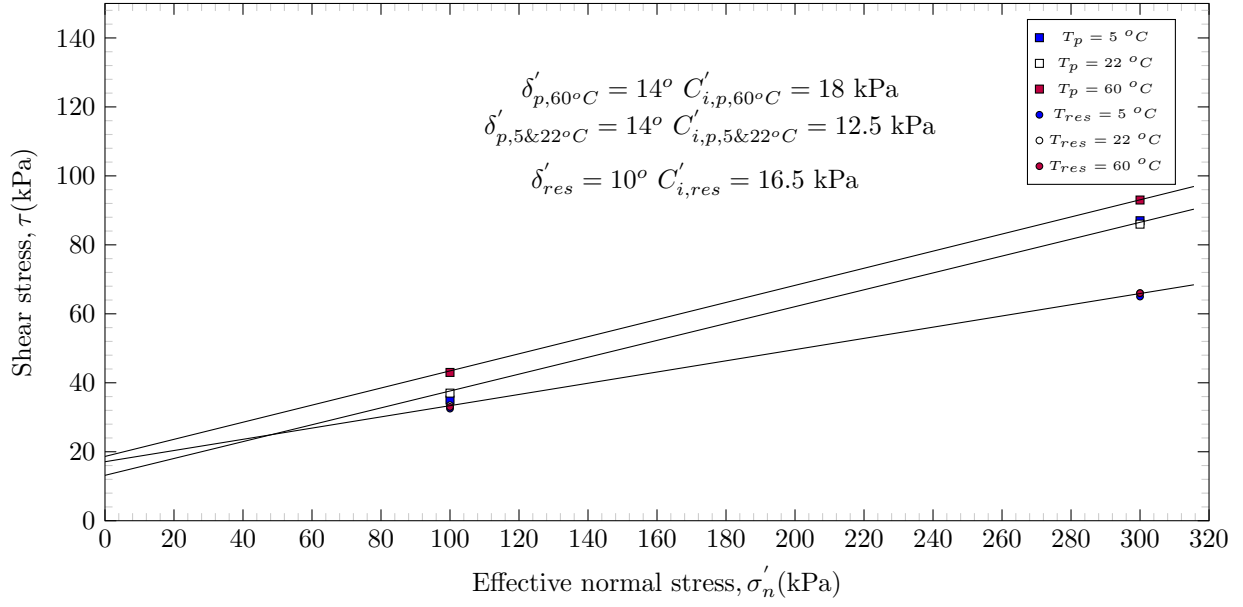


Figure 18: Shear stress vs. effective normal stress of CNL tests of clay-structure interface at $T = 5^{\circ}C$, $T = 22^{\circ}C$ and $T = 60^{\circ}C$.

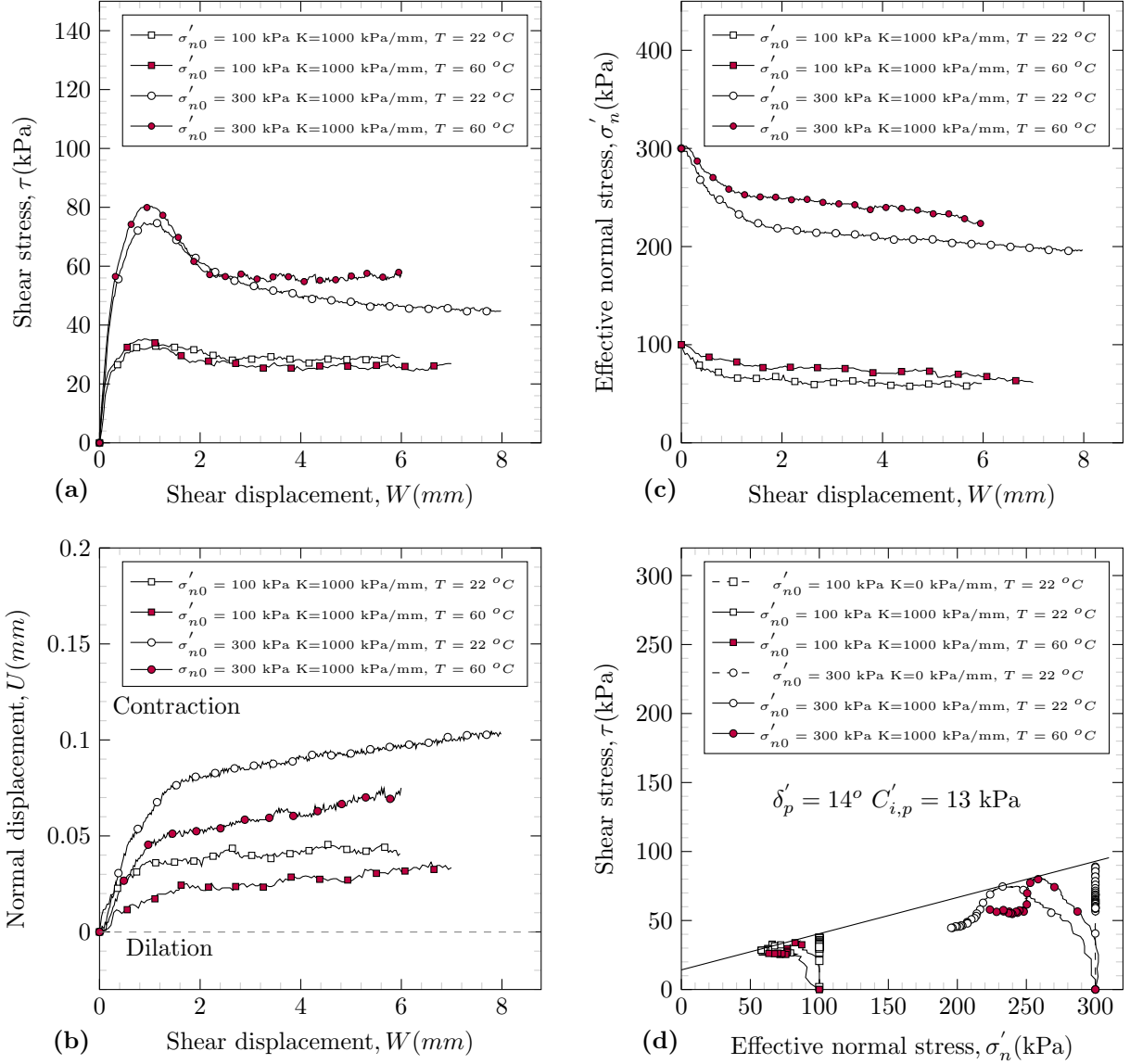


Figure 19: CNS results for clay-structure interface at $T = 22$ °C, $T = 60$ °C. (a) shear stress vs. shear displacement; (b) Normal displacement vs. shear displacement; (c) Normal stress vs. shear displacement; (d) shear stress vs. effective normal stress

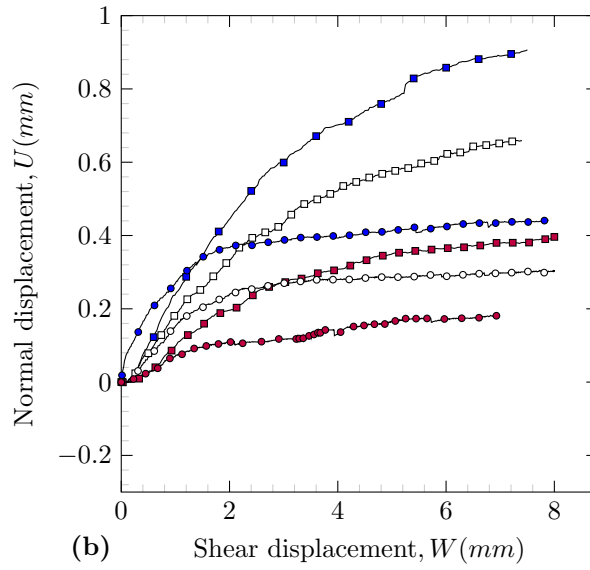
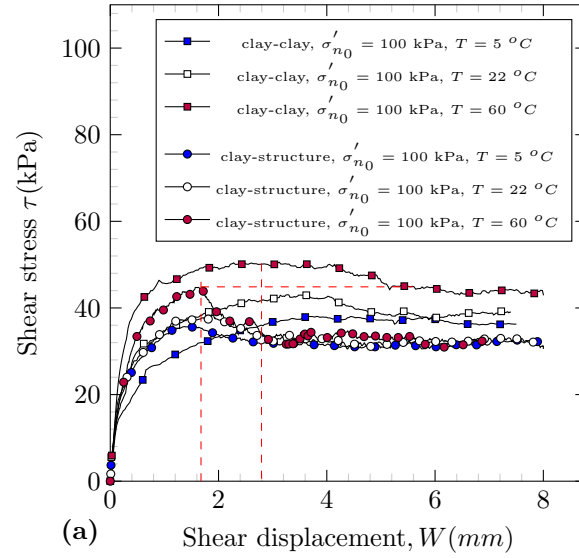


Figure 20: Comparison of CNL results for clay and clay-structure interface with $\sigma'_{n0} = 100$ kPa at $T = 5$ °C, $T = 22$ °C and $T = 60$ °C .

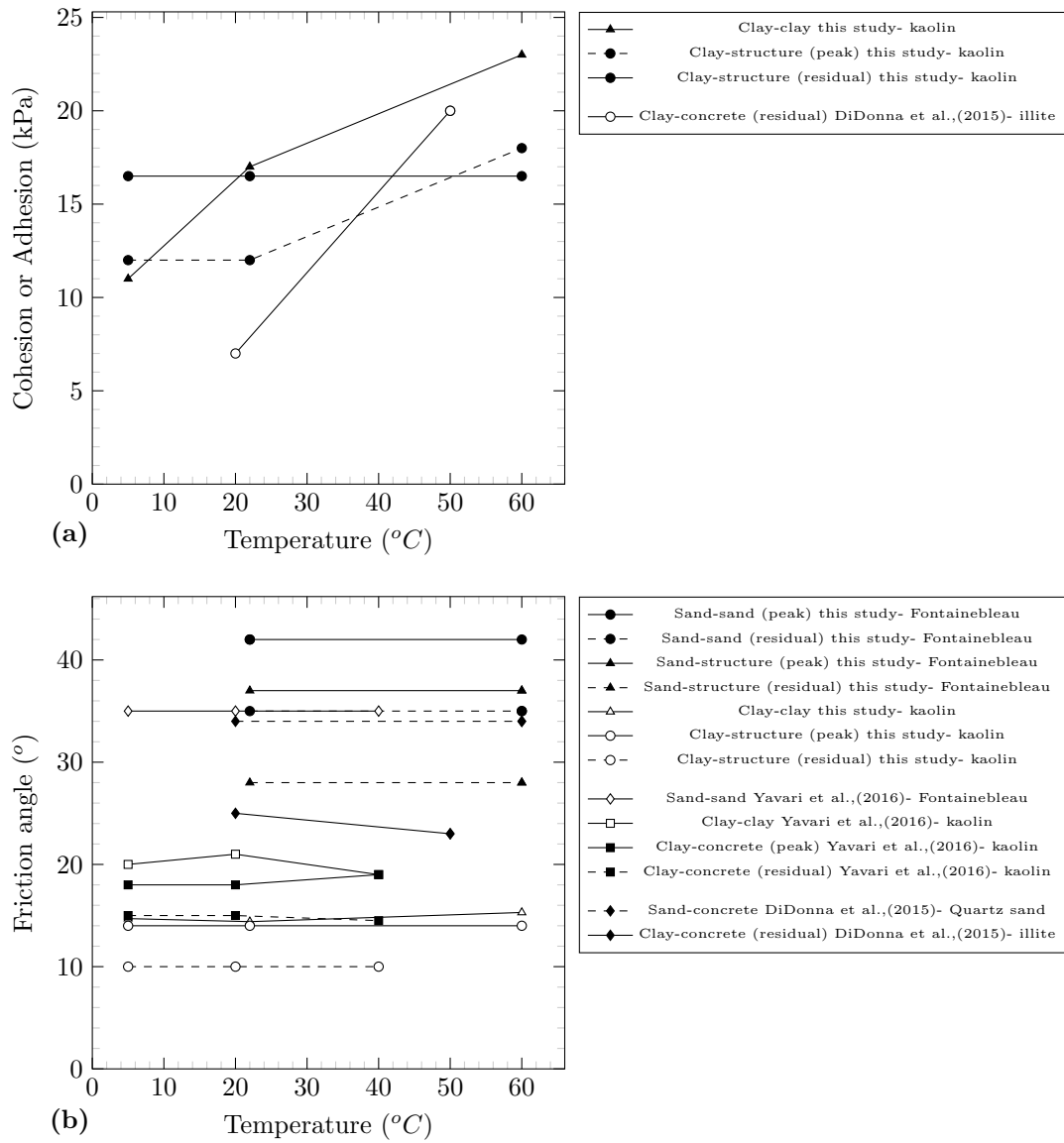


Figure 21: Effect of temperature on (a) cohesion and (b) friction angle.